Master's thesis

Designing a haptic controller for a tele-echography system

Sjamil M. Gazimagamaev

Thesis submitted for the degree of
Master in Informatics: Robotics and Intelligent Systems
30 credits

Institute For Informatics
Faculty of mathematics and natural sciences

UNIVERSITY OF OSLO

Spring 2021

Master's thesis

Designing a haptic controller for a tele-echography system

Sjamil M. Gazimagamaev

© 2021 Sjamil M. Gazimagamaev

Master's thesis

http://www.duo.uio.no/

Printed: Reprosentralen, University of Oslo

Acknowledgement

I would like to take this opportunity to express my sincere gratitude to all those who have helped me complete this project. I would first and foremost like to thank my supervisor, Kim Mathiassen, for his helpful guidance, support and encouragement. I would not have been able to complete this thesis in the same manner without his help and advice.

To my fellow students and friends, especially Song Luu, Øyvind Soma and Daniel Woldegiorgis, thank you all for the support and encouragement during this trying semester. Your support has kept me motivated!

To my family, especially my parents, thank you so much for believing, supporting and motivating me throughout my life. Fleeing from your home country, leaving behind your family and friends just so that I would be able to have this opportunity, I will forever be indebted to you.

Again, thank you everyone!

Sjamil M. Gazimagamaev

Abstract

The healthcare centers located at rural areas will have a lack of available sonographers who can perform ultrasound examinations on patients. To solve this issue and allow the patient to receive the necessary help, it is be beneficial for the healthcare centers to take into use a tele-echography system. A tele-echography system is a system based on bilateral tele-operation, meaning that the ultrasound examination is performed remotely and using force-feedback the sonographer can receive the sensation of controlling the patient's environment directly. To allow such system to operate, a communication network is used as the medium that holds the system together and allows for communication to happen between the two locations. However, when using a communication network there will be an occurrence of time-delay during the exchange of data between the locations. Time-delay will cause issues such as lengthy procedure time and inaccurate performance. Additionally, it has from previously done work been proven that delayed bilateral systems will cause instability in the system.

This thesis aims to solve these issues by designing a control architecture that will allow ultrasound examinations to be performed without time-delay being a hindrance. To limit the effects of time-delay, there exists specific control strategies that can be taken into use. One of them being the wave variable method, which transforms the power variables in the system (velocity and force) into wave variables before transmitted through the communication channel. The method is known to allow bilateral systems to maintain their stability when dealing with time-delay, but its use does not produce good tracking performance. To compensate, there can be done modifications to the method that will allow the system to produce accurate tracking performances while maintaining its stability during remote use.

To test the designed controller there was created a simplified 1-DoF Simulink model based on the controller's architecture. The model was tested with time-delay values of 200, 400, and 600 ms. The results of the simulations were found to be sufficient and give an good indication that the designed controller will allow real-world systems to produce desirable results.

Contents

List of Figures

List of Tables

Acronyms

DoF Degree of Freedom

2D 2-Dimensional

GUI Graphic User Interface

ISDN Integrated Services Digital Network

ADSL Asymmetric Digital Subscriber Line

VTHD Very High-Bandwidth Network

LAN Local Area Network

BPS Bits Per Second

ROS Robot Operating System

URDF Universal Robot Description Format

XML Extensible Markup Language

RVIZ Robot Visualization

MATLAB Matrix Laboratory

IDE Integrated Development Environment

dB Decibel

Chapter 1

Introduction

Sonography is a medical procedure that takes into use high-frequency sound waves to construct visual images of certain areas of the body, such as of the organs, blood flow, and tissues. This type of procedure is also commonly referred to as an ultrasound examination. To perform such procedure requires a sonographer who is both able to perform the examination and analyze the results based on a 2-Dimensional (2D) echographic image. The Intervention Center at Oslo University Hospital currently has a setup of a bilateral teleoperation system used for ultrasound examinations [11]. Using the setup allows the sonographer to perform the examinations without being in danger of receiving strain injuries, which they are prawned to receive due to the uncomfortable positions they have to hold the ultrasound probe with. From previously done research in regards to the strain injuries it was found that around 81% of sonographers end up receiving the injuries during their career, but dismiss the pain as they regard it being part of their work [25].

Even though using the setup allows the sonographer to perform ultrasound examinations without receiving strain injuries, it still has its limitations. To use the setup requires both the sonographer and patient to be located in same room during the examination. To bypass this limitation and extend its area of usage, the setup can by use of a communication network be extended such that the ultrasound examination can be performed while the sonographer and patient are located in two separate locations. This type of system is commonly known as a tele-echography system and has from previously done research been proven to be beneficial for both the sonographer in terms of their health and the patient's experience.

Professionals with the skill and knowledge required to perform an ultrasound examination will in most remote and isolated healthcare centers be limited. Lack of available experts may result in the patient having to either

wait for an unknown amount of time before receiving the necessary help or having to travel to a different healthcare center [9]. In case of an emergency, the patient will be limited to time and will therefore not be capable of waiting or traveling. To avoid such scenarios and ensure that the patient receives immediate help it will be beneficial for remote healthcare centers to taken into use a tele-echography system. Using a tele-echography system will allow a sonographer, located at a different healthcare center, to perform a real-time ultrasound examination on a patient located at the remote healthcare center, both in case of an emergency and regular checkup.

1.1 Previous work

In the last 20 years there has been conducted various research in the field of tele-echography. Projects such as ARTIS [29], TERESA [37], ESTELE [3] and PROSIT [10] were all started to research the benefits and usage of robot-operated tele-echography. The researchers have during these projects used their own slave-robots and master devices, where the difference between them has been in the ergonomic design of the slave robots. The systems were tested on different network infrastructures such as Integrated Services Digital Network (ISDN), 3G mobile, satellite link, and Asymmetric Digital Subscriber Line (ADSL), to evaluate the network that would optimize the system the most.

[39] presented the TER system and the results achieved by testing the system on volunteers who were located 10, 300, and 600 km from the sonographer, the conclusion of the experiments were good as there was no discomfort reported from the volunteers. This system was also tested on various networks, such as ISDN, Very High-Bandwidth Network (VTHD) and Local Area Network (LAN).

OTELO [7] took into use a pseudo-haptic fictive probe to control the positing of the remote control such that it emulated the feeling of a probe that the sonographer is used to handle. A communication software was also developed such that the system would be based upon IP protocol adapt to various networks such as ISDN, LAN, and satellite link.

Keiichiro Ito *et al.* designed a system called FASTELE which was designed to be used in a moving ambulance for cases where a trauma (FAST) exam had to be performed. The system used a mobile network called WiMAX to establish the connection with the emergency sonographer [19].

J. Seo *et al.* presented a remote ultrasound imaging system that takes into use 4G LITE connection that allows the system to be moved and used in areas where there is a mobile communication, resulting in tele-echography

being even more available for patients living in remote areas [32].

Jing Wang *et al.* designed a tele-echography system using 5G to allow sonographers to perform ultrasound examination without being in danger of contracting the Covid-19 virus [40].

Based on the descriptions of the systems above it can be seen that most tele-echographic systems contain similarities when it comes to their overall structure and purpose of use. The only obvious difference between them being the equipment, their configurations, and the medium that links the system together.

1.2 Aim of research

The aim of this thesis can be divided into two parts:

1. The Intervention Center is currently planning to extend their setup with use of 5G, such that it can be used remotely. To perform remote ultrasound examinations it is important that the communication network is reliable and efficient, therefore will one of the aims of this thesis be to evaluate 5G as a communication network and to determine if its is a suitable network to use for tele-echography.

2. There will be an occurrence of time-delay when communication network is used as the medium to transfer data between the location of the sonographer and patient. Therefore will another focus of this thesis be to design a control architecture that will allow the setup to handle the effects of time-delay during remote use, this will include looking into improved control methods, effects of time delay over the network, and modifications to the current controller that can limit the effects of the time delay.

1.3 Outline of thesis

The thesis is built up of the following chapters:

Chapter 1 will give the reader a short *introduction* of what tele-echography is and its purpose, *previous work* that has been done in the field of tele-echography, and what the *aim of the research* is.

Chapter 2 gives the reader an overview of the necessary *background theory*.

Chapter 3 contains description of central equipment for this work, giving the reader a basic understanding of their functionality and use.

Chapter 4 contains the *methodology* and will give the reader detailed information regarding the proposed control architecture and its implementation.

Chapter 5 addresses the *experiments* that were performed on both the current and proposed control architecture regarding their ability to and effects of time-delay and *results* that were found from the experiments.

Chapter 6 contains a *discussion* concerning the findings of the performed experiment.

Chapter 7 describes the *future work* that can be implemented to further the development of this work.

Chapter 8 gives a *conclusion* to the work.

Chapter 2

Background

In this chapter there will be given a thorough review of the necessary background theory needed to understand the material in regards to tele-echography, haptic and the software that was used during this work.

2.1 Tele-echography

Tele-echography is a system that takes into use the concept of tele-operation to enable the sonographer the ability of performing ultrasound examinations remotely, where tele-operation can be defined as *"extending the human capability to manipulate objects remotely by providing the operator with similar conditions as those at the remote location"* [18].

The structure of a tele-echography system is built up of two sites: *master* and *slave* site. The master site is the location of the sonographer and slave of the patient. Using a fictive probe at the master site, the sonographer sends motion commands to the slave site via a communication link. A slave-robot located at the slave site, with a probe attached to its end-effector, receives the commands which it uses to perform the motions created by the sonographer. In return are force-feedback measurement sent from slave to master site. Figure 2.1 shows a general scheme of a tele-echography system.

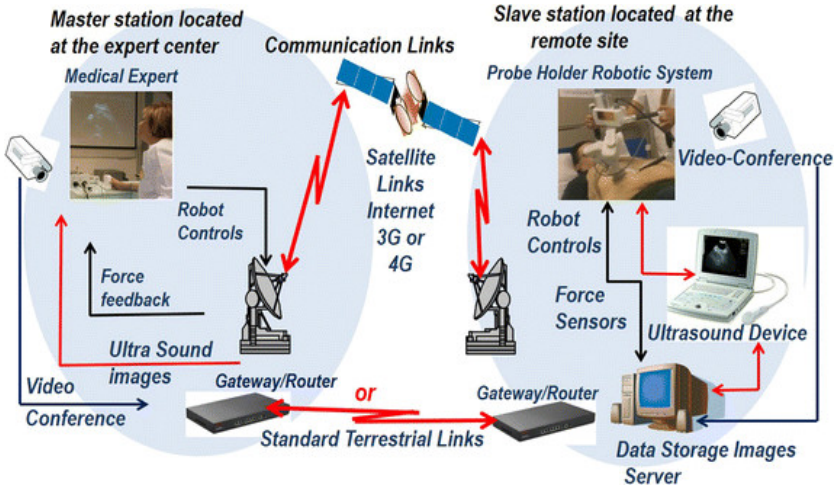

Figure 2.1: General tele-echography setup [4]

2.1.1 Master site

This is the location where the sonographer controls the overall system from. The equipment used by the sonographer will be dependent on the setup of the system, but will in most cases consist of a fictive probe and a computer workstation with a Graphic User Interface (GUI) that allows the sonographer to both communicate with their patient and receive real-time ultrasound images.

Fictive probe

The fictive probe used by the sonographer will for most tele-echography systems be a haptic device. Using a haptic device allows the sonographer to both control the robot located at the slave site and receive force-feedback, thus getting the sensation of performing the examination directly.

The type of haptic device that is used will be dependent on the system as there is not one specific device that is commonly used by all systems. For example, the haptic device used at the Intervention Center is a *Phantom Omni* by SensAble Technologies [11], while [31] took in use *Novint Falcon* by Novint Technologies. Even though the device may vary from system to system, there are a couple of factors that need to be taken into consideration when choosing the haptic device:

1. The device should have in total 6 Degree of Freedom (DoF) including 3 DoF for translations and 3 DoF for rotations. It should be able to

6-dimensional forces and torques. DoF being the number of motions that an object is able to perform.

2. The device should make it possible for the user to move the device along or rotate around one axis. They should have the capability to move the device along or rotate around any given axis.

3. The handle of the haptic device should have the functionality of being able to maintain its initial position when not being interacted with by the user. Furthermore, it should also be able to return to its initial position instinctively and steadily when released by the users grip.

   [21]

2.1.2 Slave site

This is the location where the patient, ultrasound system, and slave-robot is located at. It is also common to have a nurse beside the patient to ensure the patients safety during the examination. Likewise as at the master site, the ultrasound system at the slave site contains a GUI that allows the patient to both see and communicate with the sonographer in real-time, thus being able to receive immediate feedback and results.

Robot

The purpose of the slave-robot located at the slave site is to both hold the real probe attached to its end-effector and to execute the motion commands created by the sonographer. Likewise with the haptic device, the type of robot that is used will also vary on the setup of the system.

Joonsho Seo *et al.* used a 6-DoF robot based upon the structure of the Stewart platform, which is a parallel manipulator with 6 prismatic actuators. The probe is placed in the middle of the robot and the robot itself is during examination placed on the patient's body [33]. TER designed their robot based on both two kinematic architectures and artificial muscle actuation. Both [11] and [12] took into use the commercially available robot UR5, a robotic arm consisting of 6 DoF and 6 joints that can rotate +/- 360 degrees.

In regards to the choice of robot, there are certain requirements that have to be met to be ensure that the robot is suitable for tele-echography:

1. The most important ability that the robot should have is an inbuilt safety mechanism that allows the system to be stopped in case of a malfunction. Furthermore, the robot should also be of lightweight to further ensure the safety of the patient.

2. While not mandatory, it is recommended to use a robot that contains the same amount of DoF as the haptic device.

2.1.3 Communication link

For a tele-echography system, the medium that holds both the overall system together and allows for communication to happen between the master and slave site is a communication network. Using a communication network enables the ability to establish a communication link between two or more devices, thus allowing for transfer of data between them. For a tele-echography system, the data that is exchanged between the sites are: *ultrasound images*, *video-audio*, and *robotic control data* [38].

The systems that have been designed in the field of tele-echography over the last decades have taken into use various types of communication networks to create the necessary link, where the most commonly used networks have been *terrestrial*, *satellite*, and *wireless networks*. From the systems that were introduced in section 1.1, it can be noted that the earlier systems took into use communication wired networks such as ISDN and LAN. In the more recent years these networks have been abandoned and replaced with the likes of 4G and 5G wireless mobile networks. The reason for the change of medium is due to the capabilities of the mobile networks. To showcase the advantage of the mobile network it was by [7] conducted various experiments on their system using different types of networks. They concluded their study with mobile network being the most efficient choice as it was found to have larger mobility, lower latency, and higher bandwidth, thus resulting in a more reliable tele-echography system.

When deciding for the communication network it is therefore important that the communication network has sufficient performance capabilities in terms of parameters such as latency, bandwidth, and mobility. The necessary of requirements of the communication network for tele-echography will be given in the following section of the chapter.

2.1.4 Performance-related parameters

During this section of the chapter there will be given an overview of parameters concerning communication networks that may have an impact on the overall performance of a tele-echography system.

Time-delay

Time-delay can be defined as the total amount of time it takes for data to be sent between two or more events. In the field of tele-echography time-delay is an important factor as its occurrence during an remote ultrasound examination can lead to issues such as instability in the system, lengthy procedure time, and performance inaccuracy due to the decrease in quality of motion commands. Regarding time-delay, it was by Song Xu *et al.* conducted various experiments to both evaluate the effects of time-delay on tele-surgery systems and to find the minimum ideal time-delay to perform the procedures with. They found the ideal time-delay to be $\leq$ 200 ms, while 300 ms was found to be acceptable, but to perform procedures with time-delay over 300 ms was not advised as it was found to be too tiring and risky [41].

Time-delay will during an remote ultrasound examination occur due to mainly two reasons:

1. The first reason will be due to the distance between the two sites. By having the distance between the sonographer and patient be limited to them being in the same room, the delay that occurs under such occasion can be neglected as it will be too small to have any noticeable effect on the system. It is when the distance is greatly increased, resulting in the sonographer and patient being located in two separate locations, that time-delay will have an impact on the overall performance of the system, as the delay will increase with the distance.

2. The second reason will be due to the quality of the communication network, as its quality will have an significant impact on the amount of time-delay that will transpire. To determine the quality of a network there should be looked into its capability in terms of the parameters mentioned in section 2.1.3.

There exists mainly two types of time-delay and they can be distinguished from each other with the following descriptions of their characteristics:

1. **Constant time-delay:** Is the type of time-delay that occurs when the distance between the sites is of a large distance or when the communication happens through the use of a slow and consistent medium. As the name indicates, this type of time-delay will be constant and time-invariant, thus making it predictable.

2. **Varying time-delay:** This type of time-delay commonly occurs when the Internet is used as the communication network. The delay that

transpires with the Internet is known as latency and can be looked upon as the total amount of time it takes for data packets to travel from the sender to receiver. Due to the variation in time-delay amount and its unpredictability, systems that suffer from varying time-delay will be less stable and reliable than those with constant time-delay.

Time-delay has in previously done work greatly been taken into consideration, due to the substantial impact it will have on a system's behaviour. There has especially been conducted several research to determine the effects time-delay will have on tele-operational systems with force-feedback, also known as force-reflection. While force-feedback will give the human-operator more information to rely on, there has from previously done work been shown that a combination of force-feedback with time-delay will cause destabilization [28]. Earlier tele-operation systems did not take into use force-feedback due to this issue and it was not before late 1980, early 1990 that specific control strategies were designed to allow the systems with force-feedback to maintain their stability when dealing with time-delay [30]. The most commonly used control strategies in this regard is: *smith predictor*, *sliding mode controller*, and *wave variable method* [8].

Likewise as the control strategies, there has also been conducted research on the communication networks to determine the network that would be the most beneficial to use in terms of its ability to produce the least amount of time-delay. Pierre Vieyres *et al.* found that using Imarsat satellite lead to time delay of around 1 s, with an average variation of 200 ms [36]. Joonson Seo *et al.* used 4G with their system and found the time-delay to be 45 ms [33], while Ruizhoung Ye *et al.* found that there was no noticeable delay during the examination when using 5G as the communication network [42].

Packets and packet loss

In regards to using the Internet as a communication network, *packets* can be defined as segments that contain data and are used to send information between sender and receiver. In certain cases some of the packets may not be able to reach their destination, thus creating in *packet loss*. Packet loss usually transpires due to an overload of the communication network, resulting in some of the packets being dropped. In the context of tele-operation, packet loss will lead to the system having to operate without all the necessary information, which may lead to inaccurate performance and destabilized system. To combat the effects of packet loss, methods such as setting the missing packet to equal zero or interpolation can be used.

Jitter

Jitter is a phenomenon that occurs in the case of varying time-delay in the network. The varying time-delay will lead to the travel time of packets varying from packet to packet, leading to the packets being received in wrong orders. Commonly used approaches to handle jitter is to either use reconstruction filters that orders the packets in correct order or to distinguish them from each other with use of either time-stamps or sequence numbers. The use of the last mentioned method will in hindsight lead to use of a buffer, which may increase the delay.

Bandwidth

The amount of data that can be exchanged between two events in a given amount of time is referred to as bandwidth or data rate and is usually measured in Bits Per Second (BPS).

Network requirements

The following requirements should be met by the communication network to both avoid complications such as oscillation, delay, and instability due to the potential effects of the parameters described in this section and to ensure real-time performance during an remote ultrasound examination:

QoS	Haptics	Video	Audio	Graphics
Jitter (ms)	≤ 2	≤ 30	≤ 30	≤ 30
Delay (ms)	≤ 50	≤ 400	≤ 150	$\leq$ 100-300
Data Rate (Kbps)	512-1024	2500-40000	64-128	45-1200
Packet Loss (%)	≤ 10	≤ 1	≤ 1	≤ 10
Update Rate (Hz)	≥ 1000	≥ 30	≥ 50	≥ 30

Figure 2.2: Network requirements [24]

2.2 5G

In this section there will be given an overview of 5G in terms of its functionality, capabilities and performance rate.

2.2.1 Overview of 5G

5G is the fifth generation of mobile network and is the upgraded version of the previous networks 2 - 3 - and 4G. 5G guarantees better performance than the previous generation in terms of greater bandwidth, lower latency, and better capacity. This upgraded change in performance is due to the approach that 5G uses to send information between locations.

5G, like other wireless communication systems, takes into use radio frequencies to carry information. Unlike the previous mobile network generations, the radio frequency 5G operates on are a higher frequency called *millimeter waves*. Using millimeter waves allows a large amount of information to be carried at a faster rate than previously, thus improving the performance of the network.

The setup of 5G consists of two main components: *Core Network* and *Radio Access Network*, and have the following abilities and responsibilities:

1. Radio Access Network is built up of *small cells* and *macro cells*, these are the core of the 5G technology and allows mobile devices to be connected to the Core Network. Millimeter waves have the limitation of having a short travel distance and are easily blocked by objects. To compensate, small cells are used, which are located closely together such that the signals sent from the Macro Cells are both able to avoid objects and reach their desired locations.

2. Core Network has the task of managing all internet and data connections that are involved in the 5G technology.

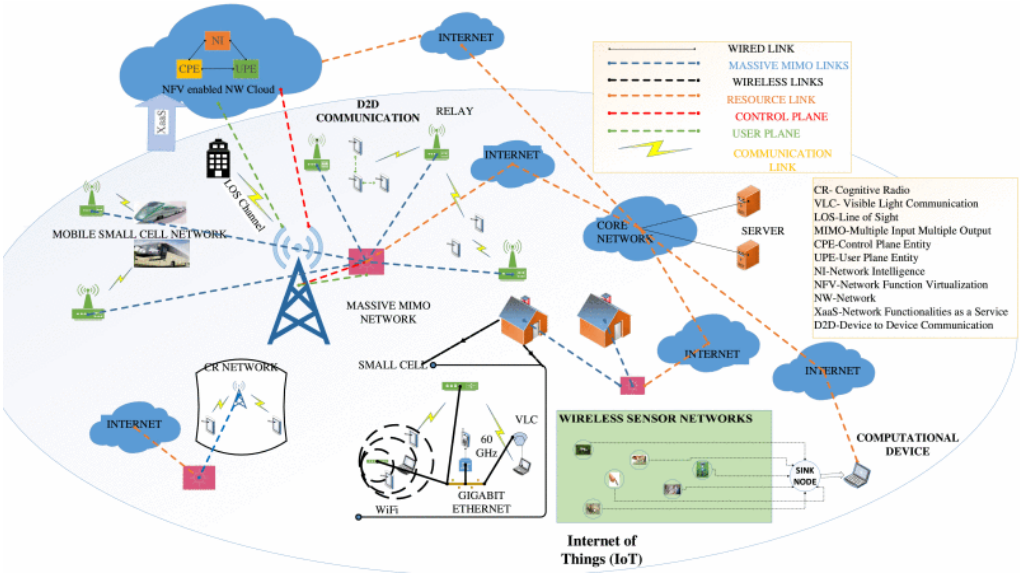

Figure 2.3: 5G mobile network structure [16]

2.2.2 Performance of 5G

In regards to the performance of 5G, there has in the last years been conducted different research to evaluate its performance compared to previous mobile network generations and other networks, where different aspects and parameters of 5G have been used as an comparison. In this section will some of the findings be presented and compared to those of 4G.

Network	Latency	Bandwidth	Average speed	Mobility
4G	30-40 ms	200-300 Mbps	25 Mbps	360 km/h
5G	1-10 ms	1-10 Gbps	200-400 Mbps	500 km/h

Table 2.1: Performance of 5G compared to 4G

It can be seen that 5G, in span of just one generation, has been able to increase the performance rate of mobile network tremendously. The increase in performance has led to mobile network being a even more efficient and reliable network to use, than previous generations.

5G has, due to its performance rate, in the recent years frequently been used as the communication network for tele-surgery and tele-echography systems [35, 23, 42]. The results gathered from its use have been positive, as it has been reported that performing procedures with 5G has led to safe and accurate performances due to factors such as its low latency and bandwidth. The sensation received when performing with 5G has been compared to that of the conventional ultrasound examination [5].

2.3 Wave variable transformation

As mentioned in section 2.1.4, one of the frequently used control strategies to limit the effects of time-delay is the wave variable method. The wave variable method was first introduced in 1989 by Anderson and Spong as the *scattering transformation* with the premise of sustaining the stability of a system with force-reflection when dealing with time-delay [2]. The method was later in 1991 further improved by Niemeyer and Slotine to make it a method suitable to be used with non-linear systems and in cases of unknown models with large uncertainties [28]. The approach that the wave variable method uses to maintain the stability of the system is by transforming the power variables (velocity and force) into wave variables, which is done with use of specific parameters and equations. In figure 4.4, a general scheme of the wave variable method can be seen.

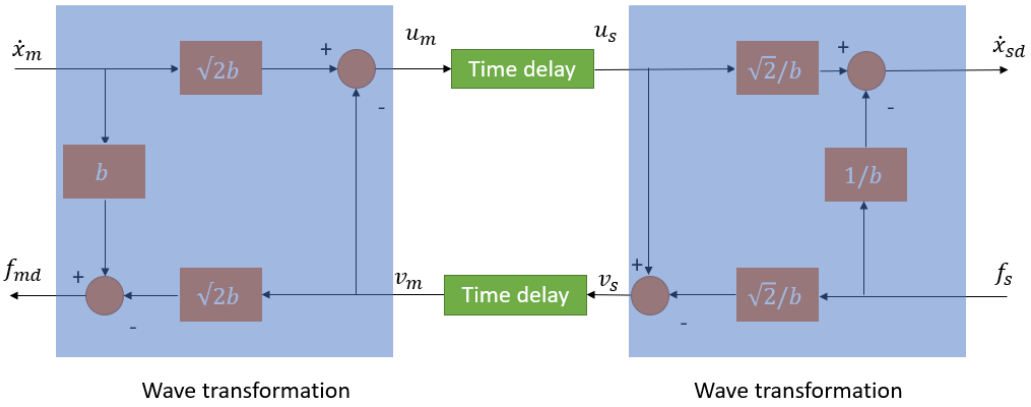

Figure 2.4: General scheme of the wave variable method

From the figure 2.4, it can be seen that the force and velocity measurements are transformed into wave variables during the exchange of data between the sites. The transformation is performed with the use of the following equations:

$$u_m(t) = \frac{1}{\sqrt{2b}}(f_{md}(t) + b\dot{x}_m(t)) \tag{2.1}$$

$$v_s(t) = \frac{1}{\sqrt{2b}}(f_s(t) - b\dot{x}_{sd}(t)) \tag{2.2}$$

$$u_s(t) = \frac{1}{\sqrt{2b}}(f_s(t) + b\dot{x}_{sd}(t)) \tag{2.3}$$

$$v_m(t) = \frac{1}{\sqrt{2b}}(f_{md}(t) - b\dot{x}_m(t)) \tag{2.4}$$

In the given equations are the parameters $\dot{x}_{sd}$ and f_{md} denoted as the velocity sent from master to slave and interaction force sent from slave to master, while f_s and $\dot{x}_m$ represents the interaction force at slave site and velocity command from the master. The parameter b is known as wave impedance and is a parameter that is tuned to modify the behavior of the system, the value of the parameter will thus be dependent on the setup of the system.

For the cases where the time delay T between the two sites is constant, can the relation of the wave variables be expressed as:

$$u_s(t) = u_m(t - T) \tag{2.5}$$

$$v_m(t) = v_s(t - T) \tag{2.6}$$

Using the previously given equation, the parameters from equations (2.1) - (2.4) can be expressed in the following manner:

$$f_{md}(t) = \frac{b}{\sqrt{2b}}(u_m(t) - v_m(t)) \tag{2.7}$$

$$f_s(t) = \frac{b}{\sqrt{2b}}(u_s(t) - v_s(t)) \tag{2.8}$$

$$\dot{x}_m(t) = \frac{1}{\sqrt{2b}}(u_m(t) + v_m(t)) \tag{2.9}$$

$$\dot{x}_{sd}(t) = \frac{1}{\sqrt{2b}}(u_s(t) + v_s(t)) \tag{2.10}$$

The power that flows into the communication blocks can likewise be expressed as:

$$P_{in} = \dot{x}_m(t)F_m(t) - \dot{x}_{sd}F_s(t) \tag{2.11}$$

An important factor when it comes to wave variables is passivity. A system is said to be passive if it does not produce any additional energy than that of what it has been given. Keeping in mind the importance of passivity and assuming that the initial energy of the system is zero, the total energy that is kept in the communication during the signal transmission between the sites can be computed as:

$$\begin{aligned} E &= \int_0^t P_{in}\tau d\tau = \int_0^t (\dot{x}_m(\tau)F_m(\tau) - \dot{x}_{sd}F_s(\tau))d\tau \\ &= \frac{1}{2}\{\int_{t-T}^t u_m(\tau)^2 + v_s(\tau)^2 d\tau \geq 0 \end{aligned} \tag{2.12}$$

From the equation can it be seen that the system is passive for any values of delay T when the delay is constant, making the system stable.

2.4 Haptic

The term haptic comes from the Greek word *haptesthai* and can be defined as *sense of touch* [17]. The concept of haptic has in the field of technology been greatly implemented and taking into use, where devices that allows its users to receive the sensation of touch when performing tasks either remotely or virtually have been created. To use the concept of haptic on devices are parameters such as force, motion, and vibration commonly used. Haptic is usually used for video-game consoles, phones, tele-operation, medicine, and robotics.

2.4.1 Haptic feedback

As previously mentioned in section 2.1.1, haptic is an important concept when it comes to tele-echography systems and is used through a haptic device that enables the sonographer to both control the slave-robot and receive force-feedback. Receiving force-feedback allows the sonographer to feel the amount of force that they are applying to the slave environment, thus resulting in them receiving the sensation of controlling the environment directly and in hindsight producing more reliable and accurate results than if the sonographer was only able to rely on visual information.

Systems that are controlled in such a manner are called bilateral systems and are said to be ideal when the amount of force felt by the human-operator

is of the same amount as that of what is applied to the slave-environment, in other words: when the system is *transparent*.

To design such a system, the concept of two-port network is commonly used. The reason being that the environment will be interacted and manipulated with through the use of two ports: the *human operator* who is located at the master site and the *slave-environment* that the human-operator will control from the master site.

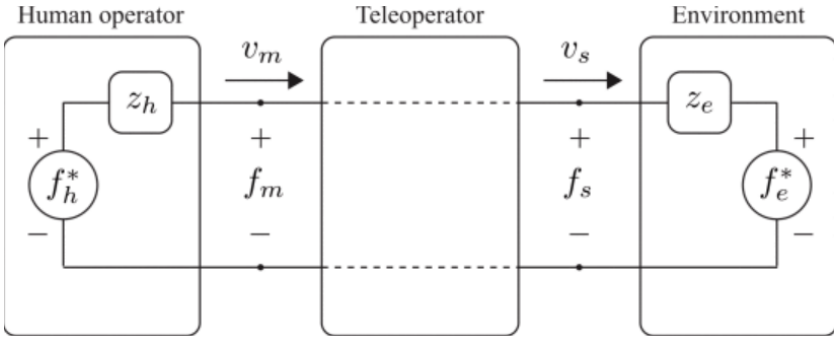

Figure 2.5: Two-port network scheme [27]

From figure 2.2, the general scheme of a two-port network can be seen. Where the variables z_h and z_e are denoted as the impedance of the human-operator and environment respectively, while f_h^* and f_e^* are the exogenous forces. To achieve transparency in such a system it is necessary that $f_m = f_s$ and $v_m = v_s$ is achieved, which in other words means that the force and velocity from the master equal that of the slave [27].

To characterize a linear two-port network equation (2.13) can be used, where the variable H is given as a 2x2 hybrid matrix and has the purpose of relating the variables, while h_{ij} are the rational functions of the Laplace variable s [27].

$$\begin{bmatrix} f_m \\ -v_s \end{bmatrix} = \mathbf{H} \begin{bmatrix} v_m \\ f_s \end{bmatrix}, \qquad \mathbf{H} = \begin{bmatrix} h_{11} & h_{12} \\ h_{21} & h_{22} \end{bmatrix} \tag{2.13}$$

A system is said to be transparent when its hybrid matrix is given as:

$$\mathbf{H} = \begin{bmatrix} 0 & 1 \\ -1 & 0 \end{bmatrix} \tag{2.14}$$

The hybrid matrix is commonly used to evaluate the level of transparency of a system.

In regards to exchange of information between master and slave site, there exists different types of port schemes that can be used based upon the amount and type of information the system exchanges. The schemes being: *one-channel*, *two-channel*, *three-channel*, and *four-channel* controller.

In the case of the system being based upon a one-way communication between the master and slave site, there will only be sent information from the master to slave. To establish such communication there is used a one-channel controller. However, the controller will not allow for haptic feedback to be received by the human-operator, as no information will be sent from the slave site.

For the case where there is a need of sending either one specific or two different types of information between master and slave site, a two-channel controller is used. The human-operator will with such controller be able to receive haptic feedback as there will be sent information back to the master from slave site.

With three-channel controller there will be sent two types of information from the master site and in return a specific type of information will be sent from the slave site. While with the four-channel controller there will be sent two types of information, both from master and slave site.

In regards to transparency when using the described controllers, it was by Edvard Naerum *et al.* found that transparency can be achieved if minimum two-channels are used and they are complimentary, meaning that force and velocity are sent in the opposite direction of each other.

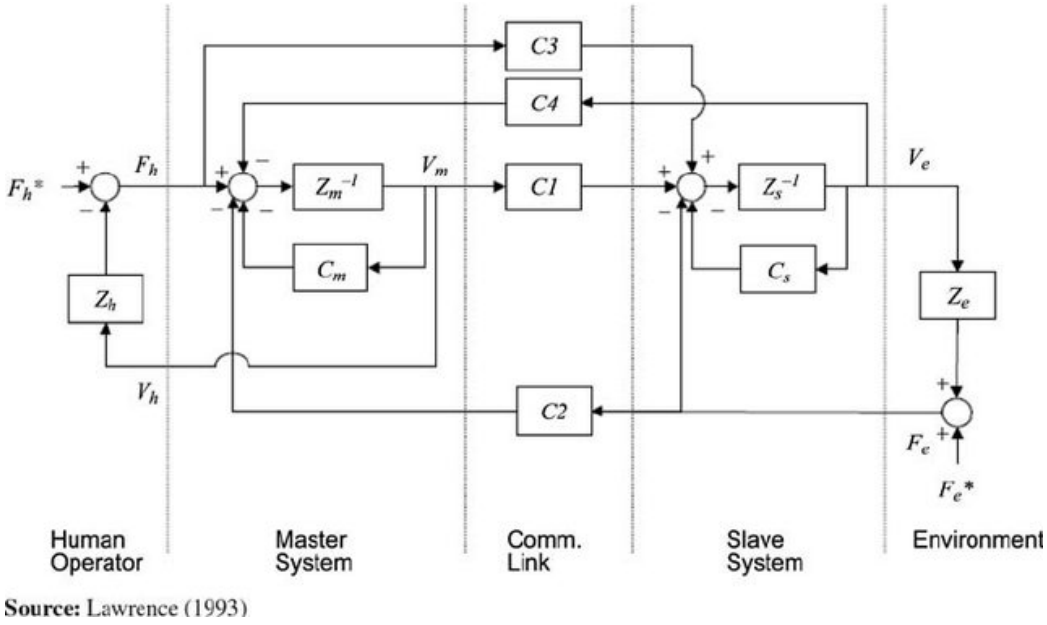

Source: Lawrence (1993)

Figure 2.6: The Lawrence Architecture [8]

In figure 2.3, the structure of a four-channel Lawrence Architecture can be seen. By following the statement given by Edvard Naerum, transparency can be achieved by either setting the gains $c1 = c2 = 0$ or $c3 = c4 = 0$. The first alternative is known as a *forward-effector* controller, while the second is referred to as the *forward-flow* controller.

When it comes to systems with either *three-channel* or *four-channel*, transparency will also be achievable as they can be complimentary.

2.4.2 Force measurement

It is, in regards to haptic feedback, important to know the amount of force that is being applied to the patient by the sonographer. This force is known as the *interaction force* and can be found by use of mainly two approaches, either by calculating an estimation or by placing a force sensor on the slave-robot's end-effector.

Force sensors, as the name indicates, are sensors that are taken into use when measuring the amount of force that is applied to a surface. There exists different types of force sensors, the most commonly used being: *resistance type*, *strain gauge*, and *piezo-electric type* [15].

1. **Strain gauge:** Are force sensors that are regularly taken in use because of their high sensitivity. The sensor is built up of a strain gauge and an

elastic element. The force is measured by the deformation that occurs of the elastic element. This deformation also causes external forces to be loaded onto the strain-gauge, which may result in overloading. To avoid this a mechanical limit must be designed. Due to this reason, it is usually difficult to design them and they also require an amplifier to be used together with it the sensor because of small signal levels.

2. **Piezo-electric type:** This type of force sensors are quite similar to that of the strain gauge, as they require an amplifier to be used together with the sensor since they require large operating voltage.

3. **Resistance type:** These are known as polymer thick film devices, with these types of sensors there will be a decrease of resistance, but an increase in the force when it is applied to the active surface.

2.5 ROS

Robot Operating System (ROS) is an open-source framework that provides its users with the ability to write robot software. It contains services that one can expect an operating system to have, such as low-level device control, message-passing between processes, hardware abstraction, and package management. ROS also provides a collection of libraries and tools that makes the process of creating and designing robot behavior across various robotic platforms simpler.

2.5.1 Nodes and topics

ROS takes into use an architecture based upon graphs to communicate, where a graph in this context can be defined as a combination of nodes and topics. Node is a process that has the purpose of executing a specific computation, while a topic can be looked upon as the gateway between two or more nodes allowing them to communicate with each other by a node either publishing information or subscribing to a topic of interest.

2.5.2 Messages

ROS takes into use a message description language to describe the data values, also known as messages, published by the nodes. By using such a description method the ROS tools are easily able to generate source code for the message type in various target languages.

2.5.3 ROS master

The ROS master provides registration and naming services to the nodes in the ROS network. It allows each node in the network to locate each other such that they can communicate with each other in a peer-to-peer manner.

2.5.4 ROS packages

The software of ROS is organized into what is known as packages. ROS packages can be seen as a collection of various files and are usually built up of supporting and executable files, which have their own individual specific purposes and usage. ROS packages are commonly used throughout the robotic community, as they allow the reuse of software by offering valuable functionality through an easy-to-understand format.

2.5.5 Catkin workspace

The workspace of ROS, also known as catkin workspace, is a workspace that allows the user to efficiently structure and organize their files, directories, source code, and resources into a ROS package, which in the process enables the possibility of code re-usability across various platforms and code sharing. The structure of the workspace is divided into several subsections containing various files based upon their purpose and type, a general structure of the workspace can be seen in figure 2.5.

```
workspace_folder/      -- WORKSPACE
 src/                  -- SOURCE SPACE
    CMakeLists.txt     -- 'Toplevel' CMake file, provided by catkin
    package_1/
      CMakeLists.txt   -- CMakeLists.txt file for package_1
      package.xml      -- Package manifest for package_1

    ...
    package_n/
      CMakeLists.txt   -- CMakeLists.txt for package_n
      package.xml      -- Package manifest for package_n
```

Figure 2.7: General catkin workspace scheme

2.6 Gazebo

Gazebo is an open-source 3D dynamic simulator that is commonly used to simulate robots in specific complex environments and is the preferred simulator to use together with ROS, as it offers a wide variety of features such as sensors, various libraries of environments and robots, numerous physics engines, and an easy to use GUI. Making it easy to test algorithms, design and simulate robots while receiving accurate and realistic results. Gazebo is also supported by Robot Visualization (RVIZ), a visualization tool that is used to visualize the state of a robot by taking into use sensor data to create a precise depiction of the robot's surroundings, allowing it to know the state of its environment.

2.7 MATLAB

Matrix Laboratory (MATLAB) is a high-level matrix-based programming language with its own Integrated Development Environment (IDE) and offers its users a wide range of libraries that commonly are used for applications such as machine learning, deep-learning, control systems, and image-and video processing.

2.7.1 Simulink

Simulink is a simulation environment that is provided by MATLAB and is commonly used for analyzing, simulating and modeling of dynamic systems. Modeling in Simulink is based on block diagrams, where its users are offered a rich library containing wide range of predefined blocks that through drag-and-drop can be utilized to create both low and high-level models. The simplicity of Simulink allows its users to both change and add to their models frequently without being in danger of causing long lasting issues or lengthening the modelling phase, thus encouraging its users to try different approaches while receiving immediate results based on their added changes. Simulink supports non-linear and linear systems and allows for models to be tested in sampled and continuous-time. Furthermore, as Simulink is incorporated together with MATLAB it is also possible to share data between the two environments.

Chapter 3

Equipment

In this chapter there will be given an overview of the equipment that was central in this work and used for the setup at the Intervention Center. The equipment consists of the haptic device Phantom Omni by Sensable Technologies and UR5 by Universal Robots.

3.1 Phantom Omni

Phantom Omni is a 6-DoF portable haptic device with a serial architecture, where a single serial chain is used to connect the handle to the housing of the device. It is manufactured by Sensable Technologies, now known as 3DSystems, and is commonly used for a wide range of applications such as tele-operation, medical, and entertainment.

The device has a workspace of 16x12x7 cm and a normal resolution of 0.055 mm. It provides its users with force feedback up to 3.3 N, where the force feedback is made available in 3-DoF and position sensing in 6-DoF.

The communication interface that is used by Phantom Omni is IEEE-1394 FireWire Port and real-time programming is accessible through the use of the OpenHaptics toolkit together with Visual C++.

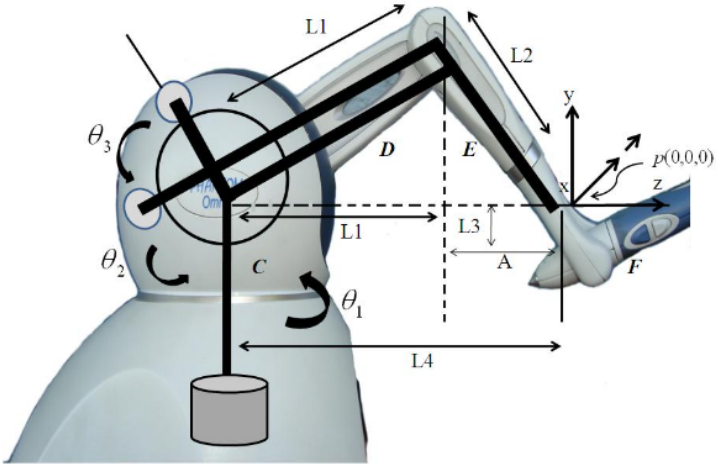

Figure 3.1: Kinematics and initial position of Phantom Omni [34]

3.2 UR5

UR5 is a 6-DoF robotic manipulator that is produced by the Universal Robots. The robot has 6 rotatable joints that can rotate -/+ 360 degrees. The kinematics of UR5 is based upon an anthropomorphic arm, where the only exception is that the last three joints of UR5 are not positioned in a spherical wrist pattern, thus allowing all six of its joints to contribute in regards to the translation and rotation motion of the end-effector.

UR5 is a lightweight manipulator with a weight of 18.4 kg, carrying capacity of 5 kg, and workspace with a radius of 850 mm. The manipulator also has an inbuilt safety mechanism and is commonly used for tasks such as placing and picking of objects and for testing purposes.

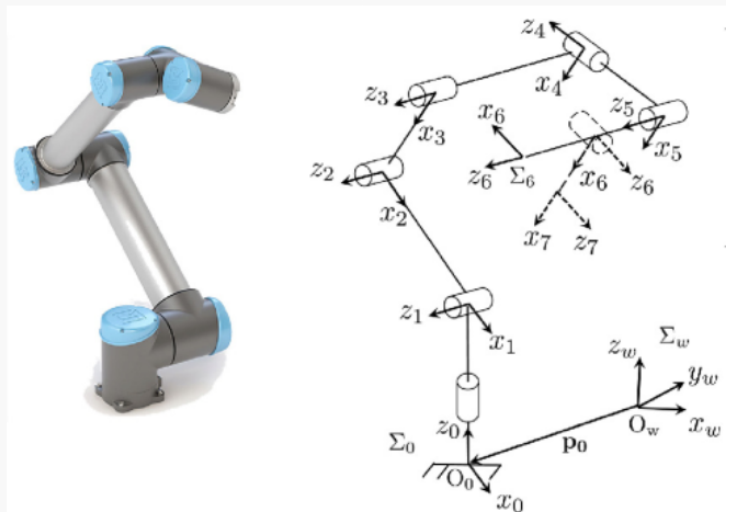

Figure 3.2: The UR5 robot [14]

As previously mentioned in section 2.2.2, force sensors are used to measure the amount of force that is applied to an environment. In the current setup at the Intervention Center, a force sensor is used to measure the force generated during the examination. The sensor is a Gamma SI-65-5 from ATI Industrial Automation and its specifications (found on ATI's website) can be seen in table 3.1, where the force variable Newton is denoted as *N*.

Calibration	F_x, F_y	F_z	τ_x, τ_y	τ_z	F_x, F_y	F_z	τ_x, τ_y	τ_z
	65 N	200 N	5 Nm	5 Nm	1/80 N	1/40 N	10/133 Nm	10/133 Nm
Sensing ranges					Resolutions			

Table 3.1: Specification of force/torque sensor

Chapter 4

Method

This chapter contains the *methodology* of this thesis. During this chapter will the development of a simulation framework using Gazebo, currently used control architecture with the setup at the Intervention Center, the proposed control architecture and its implementation in Simulink be presented in a step-by-step manner.

4.1 Simulation framework

To develop a simulation framework the open-source 3D robotic simulator Gazebo and open-source framework ROS was used. For this work would the environment at the slave site consist of the UR5 robot and the patient. The final design of the framework can be seen in figure 3.1, where the box represents the patient.

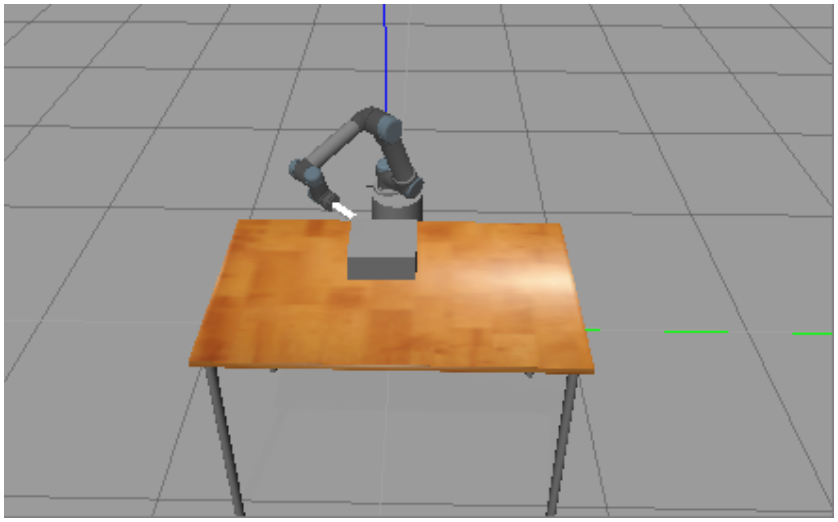

Figure 4.1: Simulation framework setup

The development of the simulation framework can be divided into three main parts, those being the following:

4.1.1 World file

The first step was to create a environment where the simulation could take place. This was achieved in Gazebo through the use of a world file, which allows world files to be created by typing the following command in a command prompt:

Gazebo

Executing the command leads to Gazebo activating and an empty world file, containing open space, being created. Using the world file, Gazebo enables its users to design their ideal environment by modifying and adding to it based upon the criteria they wish to meet. In designing the environment can either premade or default models be taken into use. Certain types of the models are made available by Gazebo, such as the box and table in figure 3.1. The models offered by Gazebo can be accessed in the *insert* section under *models.gazebosim* category. The settings of the included models, such as their size, physics, and pose, can also be regulated and altered with the use of *edit model* option.

The last step of designing the environment was to save the file as it has to be accessed again later in the process. Saving a world file is done by giving it a specific file name and saving it as a world file type (e.g. world1.world).

4.1.2 UR5

As mentioned, some of the necessary models may not be provided by Gazebo and will therefore have to be designed and created by the user. Creating a model can be done using different methods, where the most common approach is to create an Universal Robot Description Format (URDF) model, which was the method used in this work.

For the simulation framework that was to be created in this work there was a need for a UR5 robot model. As Gazebo did not provide such model in their library it was necessary to either create it using URDF or download a existing model from the Internet. In this work it was chosen to use the *universal robots* package made available by ROS, which contains models of the universal robots (UR3, UR5 and UR10) and are all functional in Gazebo.

To access the package, the installation process described on the ROS website was followed:

`http://wiki.ros.org/action/show/universal_robots?action=show&redirect=universal_robot`

Once the package was installed, a launch file was created for the robot. A launch file is a file that gives a detailed description of the robot and contains information such as its starting pose, the world file that the robot is going to be launched in, and re-directions to other files that contain more information about the robot.

```
<?xml version="1.0"?>
<launch>
  <arg name="limited" default="false"  doc="If true, limits joint range [-PI,
PI] on all joints." />
  <arg name="paused" default="true" doc="Starts gazebo in paused mode" />
  <arg name="gui" default="true" doc="Starts gazebo gui" />

  <!-- startup simulated world -->
  <include file="$(find gazebo_ros)/launch/empty_world.launch">
    <arg name="world_name" default="$(find master_gazebo)/worlds/
ur5_test_world.world"/>
    <arg name="paused" value="$(arg paused)"/>
    <arg name="gui" value="$(arg gui)"/>
  </include>

   <!-- send robot urdf to param server -->
  <include file="$(find master_description)/launch/master_upload.launch">
    <arg name="limited" value="$(arg limited)"/>
  </include>
  <!-- push robot_description to factory and spawn robot in gazebo -->
  <node name="spawn_gazebo_model" pkg="gazebo_ros" type="spawn_model"
        args="-urdf -param robot_description -model master_robot -z 1.0
           -J elbow_joint 1.5
           -J shoulder_lift_joint -1.22
           -J shoulder_pan_joint -0.75
           -unpause"
        output="screen" />

  <include file="$(find master_gazebo)/launch/controller_utils.launch"/>
```

Figure 4.2: UR5 launch file

4.1.3 End-effector

As of the date, this thesis was written, were there no end-effector tools included with the robots from the universal robots package. There exist some models on the internet that can be installed and attached to the robot manually, such as the *robotiq gripper*, but otherwiser the model has to be designed and created by the user.

In his work the tool that was going to be attached to the robot's end-effector was a probe. To create such a tool the mentioned URDF model method was used, which is a ROS package that allows models to be created by manually writing a description of the models properties such as its links, joints, visual, and collision matrices using Extensible Markup Language (XML) style.

There exists different types of files in the universal robots package, all with their own specific purposes and specifications. One of those files is a URDF file called *ur5_ upload*, which gives a default description of the UR5 robot. To create the probe tool, the content of the file was copied and a new file called *master_ upload* was created. In the master_upload file, the description of the tool was written, where a link *end_ effector* and joint *end_ effector_ tool* was created. The link describes the visual, physics, and geometry of the tool, while the joint is used to add the tool (child link) to the end-effector (parent link) of the robot.

```
<link name="end_effector">
  <inertial>
      <mass value="1000" />
      <origin xyz="0.0 0.0 0.0" rpy="0 0 0" />
      <inertia ixx="0.01" ixy="0" ixz="0" iyy="0.01" iyz="0" izz="0.01" />
  </inertial>
  <visual>
      <geometry>
         <box size="0.15 0.03 0.02"/>
      </geometry>
      <material name="White" />
  </visual>
  <collision>
      <origin xyz="0.0 0.0 0.0" rpy="0.0 0.0 0.0" />
      <geometry>
         <box size="0.15 0.03 0.02"/>
      </geometry>
  </collision>
</link>

<joint name="end_effector_tool" type="fixed">
  <parent link="ee_link" />
  <child link= "end_effector" />
  <origin xyz="0.045 0.0 0.009" rpy="0.0 0.0 0.0" />
</joint>

</robot>
```

Figure 4.3: URDF file for end-effector tool

Once the URDF file of the robot and the tool was created, the path of the file was included in the launch file description such that when the robot was to be launched in Gazebo it would be launched with the tool attached to the robot's end-effector.

4.2 Current controller

In this section of the chapter there will be given an overview and description of the current control architecture, as it in the following sections will be used to compare against the proposed control architecture, both in terms of their differences in structure and their performance results when tested with added time-delay. The current controller will be presented by first giving a summary of its functionality before the components its built up of is showcased and described in a detailed manner.

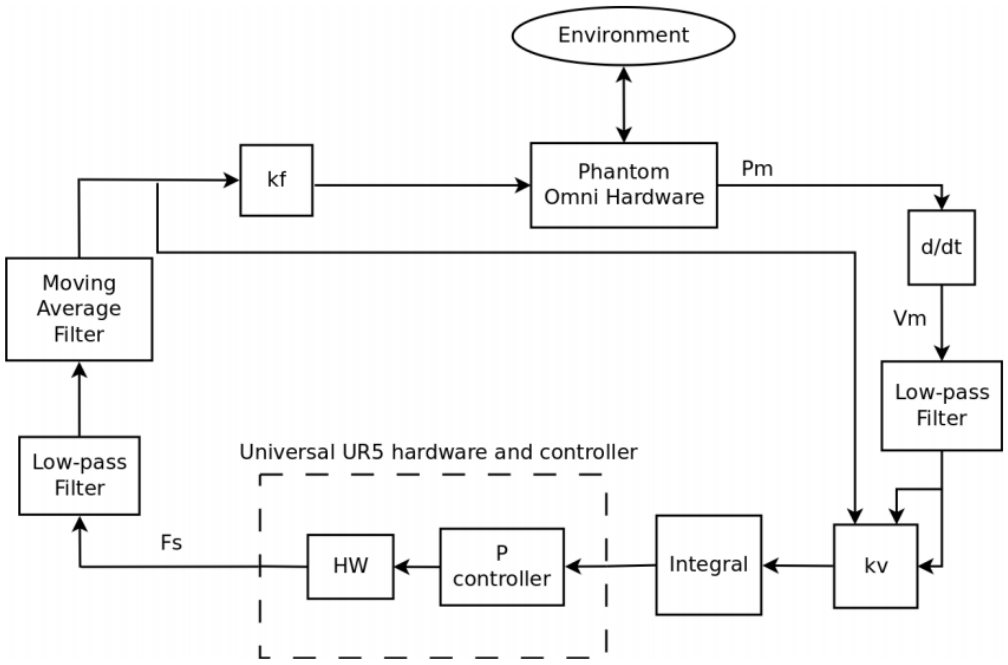

Figure 4.4: The current controller [11]

Functionality

Figure 4.4 shows the architecture of the current controller. From the figure it can be seen that the control of the system starts at the master site with the sonographer applying a certain amount of force to the haptic device, Phantom Omni. The device then sends the position commands P_m to the slave site, which are by use of derivation transformed into velocity and filtered for noise with a *low-pass filter*. The velocity measurements are at the slave site received and scaled with a scaling factor k_v. The scaled measurements are integrated and used together with the inverse kinematics of UR5 to obtain the desired joint positions q. To follow the desired joint positions is a P-

controller, with a gain of P, used. Using a force sensor, the interaction force f_s is measured, reduced of noise with both a low-pass and moving average filter, scaled with a scaling factor k_f and delivered to Phantom Omni.

Network model

As mentioned in section 2.2.1, a bilateral tele-operation system can be modelled after a two-port network model, which is the model that the current controller has based it architecture on. The controller takes into use the forward-flow Extended Lawrence Architecture by sending velocity commands from master to slave site and measured interaction force from slave to master site. Due to the fact that there only is one specific power variable being sent between the two sites it can be noted that the controller is complementary, thus allowing the system to be transparent.

Filtering

Filtering is implemented into the control architecture to reduce the noise that will occur during the use of the system. Systems that are tele-operated by a human-operator will commonly consists of low frequencies, whereas high frequencies will be an indication of noise. Regarding this issue, it was by CJ Zandsteeg *et al.* found that to achieve good position tracking it is necessary to have up to 2 Hz while any frequencies above 8 Hz should be suppressed [43].

Unwanted noise for this particular system will occur due to the following reasons:

1. The UR5 robot will in the case where it is not being controlled by the sonographer look motionless, but due to gravity compensation it will in reality try to adjust its joints. The adjustment and motions caused by its motor will result in forces being detected by the force sensor, resulting in vibration noises being created.

2. The sonographer will have difficulties when it comes to holding the haptic device still at a certain position for a long period of time. This also will result in vibration noises being created from the haptic device.

To reduce the amount of noise that may transpire due to the reasons given above, it is necessary to take into use a low-pass filter. Low-pass filter, as the name may indicate, is a filter that filters out high frequencies by only allowing frequencies of lower domain to bypass. As noise are made up of high

frequencies, the use of a low-pass filter will result in the noise greatly being reduced, thus resulting in a more accurate performance of the system.

For the current setup, a low pass filter with a cut-off frequency of 55 Hz and a period of 3 samples is taken into use. Additionally, a moving average filter of 3 samples is used to reduce the additional noise developed from the force readings.

Gain compensation

As mentioned in section 1.1, it is important that the sonographer during an ultrasound examination is able to avoid receiving strain injuries. In the case the examination is performed with the use of a tele-operational system and there is full transparency in the system, there will still be a possibility of the sonographer receiving strain injuries, as full transparency will equal that of the sonographer holding the probe themselves. Full transparency in the system will therefore diminish an important purpose of using tele-operation system to perform ultrasound examinations. To bypass such issue, it is by the current setup used two scaling factors k_f and k_v. k_f scales the force measured at slave site, while k_v scales the Cartesian velocity sent from master to slave site. To avoid full transparency, the scaling factors are typically given a value of $k_f = k_v < 1$.

4.3 Design of new controller

In this section of the chapter the proposed control architecture will be presented. The main motivation and premise during the design process was to extend the current control architecture by making it suitable for tele-echography use in terms of being able to handle effects of time-delay and other parameters.

4.3.1 Limiting the effects of time-delay

To compensate for the potential time-delay, the wave variable method from section 2.1.5 was taken into use. The wave variable method was chosen in this work since it is easy to implement into control schemes and does not require any knowledge on the amount or type of time-delay. The method has since its first introduction in 1989 been evaluated and experimented on to determine its usability when used together with bilateral systems. In the previously done work, it was found that the stability of the system was preserved, but the tracking performance and force command results were found to be poor

[44]. It was additionally found that when used in circumstances with varying time-delay, T = T(t), would result in the passivity of the system no longer being upheld, thus destabilizing the system.

$$u_s(t) = u_m(t - T_1(t)) \tag{4.1}$$

$$v_m(t) = v_s(t - T_2(t)) \tag{4.2}$$

Equation (4.1) and (4.2) shows the wave variable transformation in case of varying time-delay, where *T1* and *T2* is denoted as the varying time-delay in forward and backward path. Implementing the equations (4.13) - (4.14) into previously given equation (2.12), gives:

$$\begin{aligned}\int_0^t P_{in}\tau d\tau =& \frac{1}{2}\left\{\int_{t-T_1(t)}^{t} u_m(\tau)^2 + \int_{t-T_2(t)}^{t} v_s(\tau)^2 d\tau\right. \\ &- \int_0^{t-T_1(t)} \frac{T_1'(\sigma)}{1-T_1'(\sigma)} u_m(\sigma)^2 d\sigma \\ &\left.- \int_0^{t-T_2(t)} \frac{T_2'(\sigma)}{1-T_2'(\sigma)} v_s(\sigma)^2 d\sigma \right\}\end{aligned} \tag{4.3}$$

The parameters σ and T_i' are expressed as $\sigma = \tau - T_i(\tau) := g_i(\sigma)$ and $T_i'(\sigma) := \frac{dT_i}{d\tau}|_{\tau=g^{-1}(\sigma)}$

In equation (4.3), it can be seen that the last two terms will in the of increasing delay be non-positive, making the system not passive.

To sustain the passivity of the system in varying time-delay cases, the approach proposed by Chopra *et al.* was taken into use. They suggested that to uphold the passivity of the system time-varying gains f_i should be implemented [22], such that the relationship of wave variables can be expressed as:

$$u_s(t) = f_1(t)u_m(t - T_1(t)) \tag{4.4}$$

$$v_m(t) = f_2(t)v_s(t - T_2(t)) \tag{4.5}$$

The passivity of the system with time varying gains implemented can be proven by inserting equation (4.4) - (4.5) into equation (2.12):

$$\int_0^t P_{in}\tau d\tau = \frac{1}{2}\left\{\int_{t-T_1(t)}^{t}(u_m(\tau)^2 + \int_{t-T_2(t)}^{t} v_s(\tau)^2 d\tau - \int_0^{t-T_1(t)} \frac{1-T_1'(\sigma)-f_1^2}{1-T_1'(\sigma} u_m(\sigma)^2 d\sigma - \int_0^{t-T_2(t)} \frac{1-T_2'(\sigma)-f_2^2}{1-T_2'(\sigma})v_s(\sigma)^2 d\sigma\right\} \tag{4.6}$$

By choosing the time-varying parameter to be f_i^2 it will result in the second terms being eliminated, making the system passive. The passivity can also be preserved when the condition of the gains are set to be:

$$f_i^2 \leq 1 - \frac{dT_i}{dt}; i = 1, 2 \tag{4.7}$$

Using time-varying gains will lead to the system being passive, thus being stable, but the system will still produce poor tracking performance and force command results. To both sustain the stability of the system and increase its overall performance, it was by Chopra *et al.* suggested to also implement a feed-forward controller together with the time-varying gains.

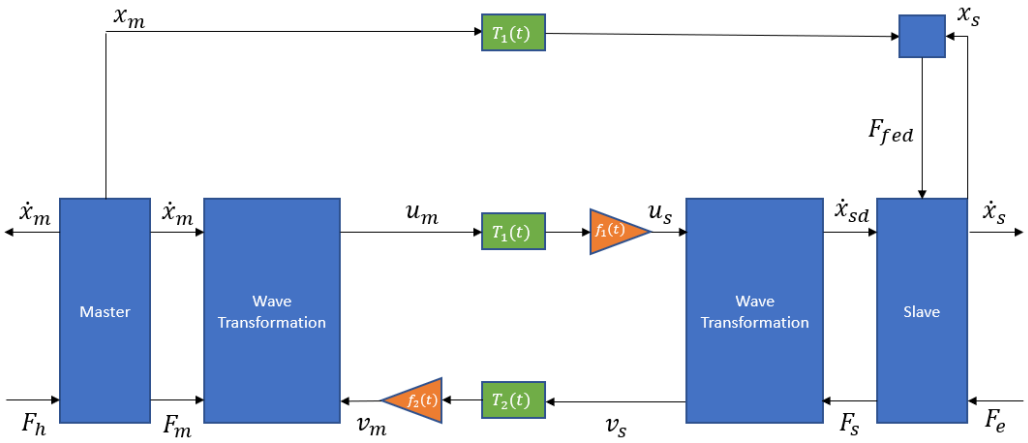

Figure 4.5: Wave variable with feed-forward controller

In figure 4.6, the suggested control architecture with the feed-forward controller can be seen. The feed-forward value can be calculated using the following equation:

$$F_{fed} = K_{fed} \cdot e_{fed} \tag{4.8}$$

Given the dynamics of the master and slave:

$$\begin{aligned} M_m\ddot{x}_m + B_m\dot{x}_m &= F_h - Fm \\ M_s\ddot{x}_s + B_s\dot{x}_s &= F_{fed} + F_s - F_e \end{aligned} \tag{4.9}$$

The value of K_{fed} should be chosen such that $0 < K_{fed} < \sqrt{2B_s}$, where B_s is given as the damping constant of the slave-robot and the position tracking error e_{fed} can be found using $e_{fed} = x_m(t - T_1(t)) - x_s(t)$.

Even though the system with a feed-forward controller implemented gave good results, it was by Olga *et al.* suggested to also implement a feedback controller to further improve the tracking performance and force command results [20]. Similar to the feed-forward controller, the equation for feedback controller can be given as:

$$F_{back} = K_{fed} \cdot e_{back} \tag{4.10}$$

Where $e_{back} = x_s(t - T_2(t)) - x_m(t)$

Implementing the feedback controller gives the following and final dynamic equations of the master and slave:

$$\begin{aligned} M_m\ddot{x}_m + B_m\dot{x}_m &= F_{back} + F_h - Fm \\ M_s\ddot{x}_s + B_s\dot{x}_s &= F_{fed} + F_s - F_e \end{aligned} \tag{4.11}$$

Some of the equations that were introduced in this section will only apply for systems of 1-DoF. Since the setup at the Intervention Center is of multi-DoF, certain parameters and equations will have to be expressed in the following way:

The haptic device Phantom Omni only operates on 3-DoF, thus resulting in the velocity, force, and wave impedance variables having to be expressed in the same amount of DoF:

$$\underline{\dot{x}}_{sd} = \begin{bmatrix} \dot{x}_{sd} \\ \dot{y}_{sd} \\ \dot{z}_{sd} \end{bmatrix}; \underline{\dot{x}}_m = \begin{bmatrix} \dot{x}_m \\ \dot{y}_m \\ \dot{z}_m \end{bmatrix}; \underline{F}_s = \begin{bmatrix} F_s^x \\ F_s^y \\ F_s^z \end{bmatrix}; \underline{F}_m = \begin{bmatrix} F_m^x \\ F_m^y \\ F_m^z \end{bmatrix} \tag{4.12}$$

$$B = \begin{bmatrix} b_x & 0 & 0 \\ 0 & b_y & 0 \\ 0 & 0 & b_z \end{bmatrix} \tag{4.13}$$

Regarding the wave transformation equations that were expressed in equations (2.1) - (2.4), it was by Munir *et al.* recommended to express them in the following manner for a multi-DoF system [26]:

$$\begin{aligned} \underline{u}_s &= A_w \underline{\dot{x}}_{sd} + B_w \underline{F}_s \\ \underline{u}_m &= A_w \underline{\dot{x}}_m + B_w \underline{F}_m \\ \underline{v}_s &= C_w \underline{\dot{x}}_{sd} - D_w \underline{F}_s \\ \underline{v}_m &= C_w \underline{\dot{x}}_m - D_w \underline{F}_m \end{aligned} \tag{4.14}$$

The variables A_w, B_w, C_w and D_w are given as scaling matrices of size $(n \times n)$, where n is the DoF of the system. $\underline{u}_s$, $\underline{u}_m$, $\underline{v}_s$ and $\underline{v}_m$ are vectors of size $(n \times 1)$.

4.3.2 Proposed control architecture

Taking into consideration the factors and approaches that were presented and discussed in this section, the following control architecture was designed:

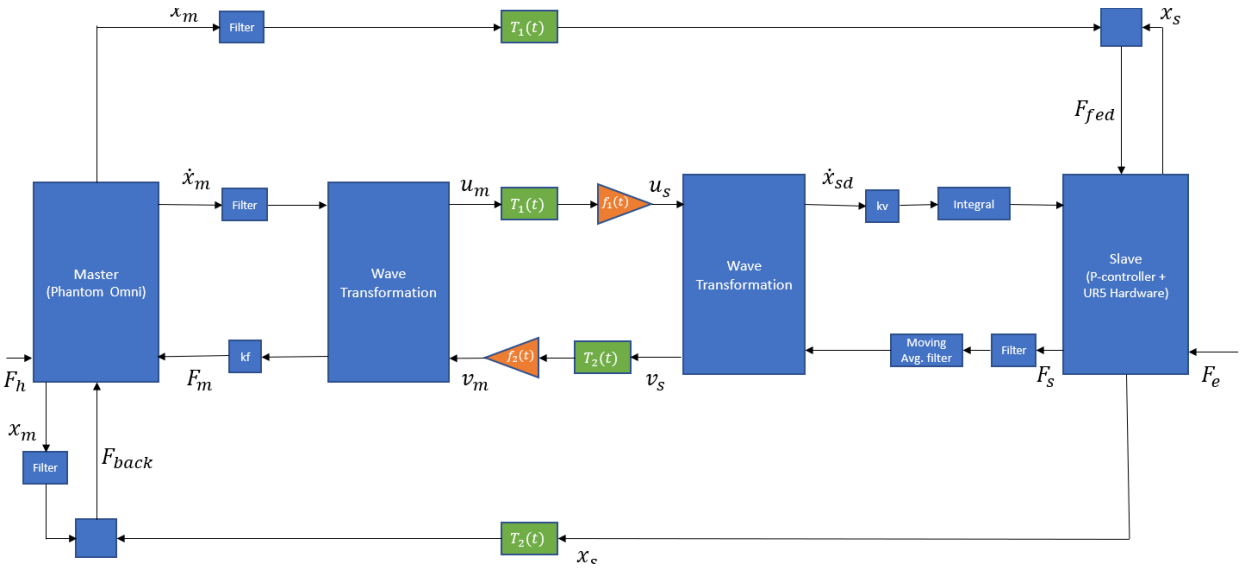

Figure 4.6: The proposed control architecture

From figure 4.6 it can be seen that the proposed control architecture shares similarities with the current control architecture from figure 4.4. This is because the wave variable method is a control strategy that is easy to implement into existing control schemes, allowing the system to operate as previously while additionally being able to handle the effects of time-delay.

The following choices were made for the filtering and network model in the proposed control architecture:

Network-model

For the network model of the controller it was chosen to further use the two-port forward-flow architecture due to the following reasons:

1. Using a forward-flow controller will allow the sonographer to receive force-feedback measurements from the slave site, which is important as it will allow the sonographer to get the sensation of controlling the slave environment directly.

2. Since the current setup is going to be extended using 5G mobile network will the fact that the controller only consists of two communication channels results in a minimum need of bandwidth. This may in hindsight increase the performance of the system as the delay will be limited to two channels.

3. Wave variable method is commonly used with systems that exchange the power variables velocity and force [1], it was therefore convenient to continue using the forward-flow controller.

Filtering

The low-pass filter that is implemented and used with the current controller has from its use shown to be able to reduce most of the occurring noise in the system [11]. Due to its sufficient performance it was chosen to continue using it with the new control architecture, together with the moving average filter. Another approach that would have been appropriate to consider for the proposed controller would be the findings of [13]. They found that using a Butterworth low-pass filter with a cutoff frequency of 1 Hz at -3 Decibel (dB) and 5 Hz at -25 dB resulted in most of the noise in the system being reduced.

4.4 Implementation of the controllers

It was initially planned to take into use the developed simulation framework from section 4.1 together with the haptic device Phantom Omni for the implementation and testing of both the current and proposed control architectures. The simulation framework was going to be used to evaluate both the current and proposed control architecture's ability to handle effects of time delay. Furthermore, it was planned to use Phantom Omni to test the control performance of the proposed controller while receiving force-feedback. But due to lack of necessary equipment, this implementation was not achievable. To compensate, it was decided to perform a simplified implementation of the controllers using Simulink.

4.4.1 MATLAB and Simulink

As mentioned in section 2.6.1, Simulink is a simulation environment that is provided and incorporated with MATLAB and allows for easy modelling through the use of its drag-and-drop block library. In this work, the R2020a version of MATLAB was used via a Windows operated PC. The system requirements of the particular version of MATLAB for Windows and other operating system can be found on MATLAB's website, MathWorks:

`https://se.mathworks.com/support/requirements/previous-releases.html`

Before performing the implementation, there was first created a simplified 1-DoF control architecture design for each of the controllers. The control architectures can be seen in figure 4.7 and 4.8, it can be noted that due to their simplifications, factors such as noise and scaling of the power variables have been neglected. After creating the simplified control architectures, there was established two separate environments in Simulink to give the controllers each their individual work environments. Using the block library provided by Simulink and selecting the necessary blocks, there was created two Simulink models of the controllers using the control architectures from figure 4.7 and 4.8 as reference. In the following section there will be given a description of the blocks that were used, their set specifications and the final Simulink models of the controllers will be showcased.

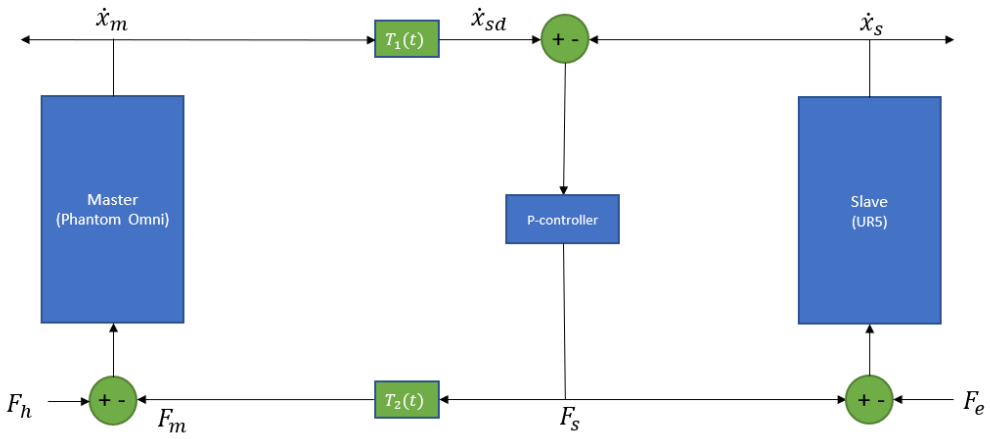

Figure 4.7: Simplified control architecture representing the current controller

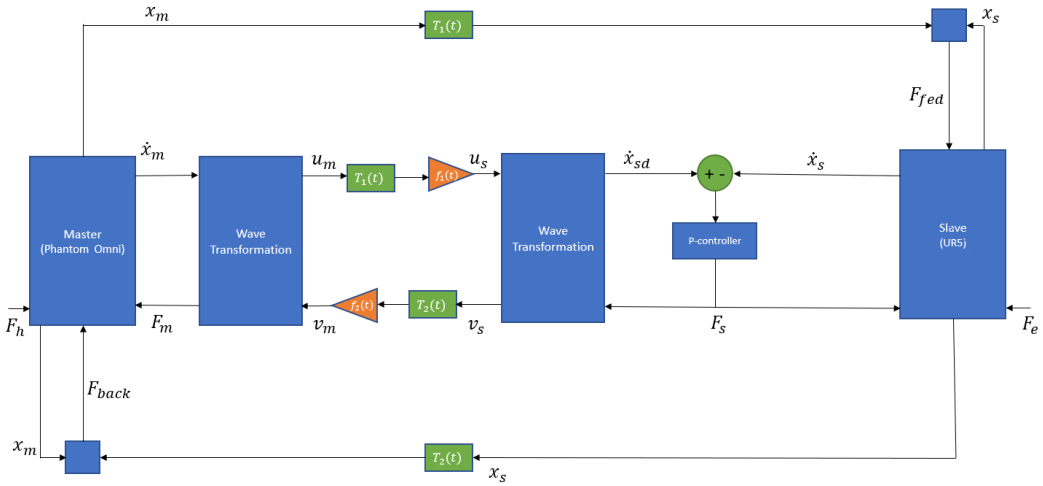

Figure 4.8: Simplified control architecture representing the proposed controller

4.4.2 Blocks

Sine Wave
To send velocity and force measurements between master and slave, the sine wave block was used. The signal created by the block represents the force applied by the sonographer and measured interaction force at slave site.

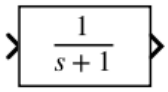

Transfer function
To represent both the haptic device Phantom Omni and slave-robot UR5, the transfer function block was used. The dynamic parameters for Phantom Omni was set to $M_m = 0.1$ and $B_m = 2$, while for the UR5 they were set to $M_s = 1$ and $B_s = 2$.

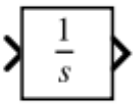

Integrator
Since both the haptic device and slave-robot will output velocity measurements, a integrator block was used to find their respective positions.

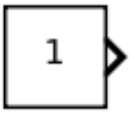

Constant
Used to specify a specific value.

Random Number
Produces a uniformly distributed random number between two specified interval values.

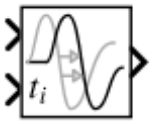

Time-delay
The time-delay block was used to add time-delay into the system, allowing for tests to performed to evaluate the controllers performance in terms of handling effects of time-delay. The block, as can be seen on the image, consists of two inputs. The upper input is preserved for inputs such as velocity and force measurements, while the second input is used to declare both the amount of delay and whether the system is tested for constant or varying time-delay. In the case of constant time-delay, a constant block with a specific value can be used, while for varying time-delay can the random number block be applied.

P-controller
The proportional controller was added to the system using the PID block, which allows the user to select between a P, PI or PID-controller. The value of gain P was for this particular system set to 300, which was found through the use of trial-and-error method where different value of P was tested on the system and the value that produced the most desirable outcome was chosen.

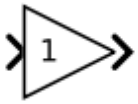

Gain
In the case of the proposed controller, the gain block was used to implement the wave impedance values b, $\sqrt{2b}$, $\sqrt{2/b}$ and $1/b$ and varying gains f_i

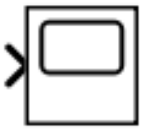

Scope
To evaluate the results produced by the system, a scope block was utilized, which presents the results in a graph-like manner.

Using the described blocks together with their set specifications and modelling the models after the simplified control architectures from figure 4.7 and 4.8, the following Simulink models were created:

Current controller

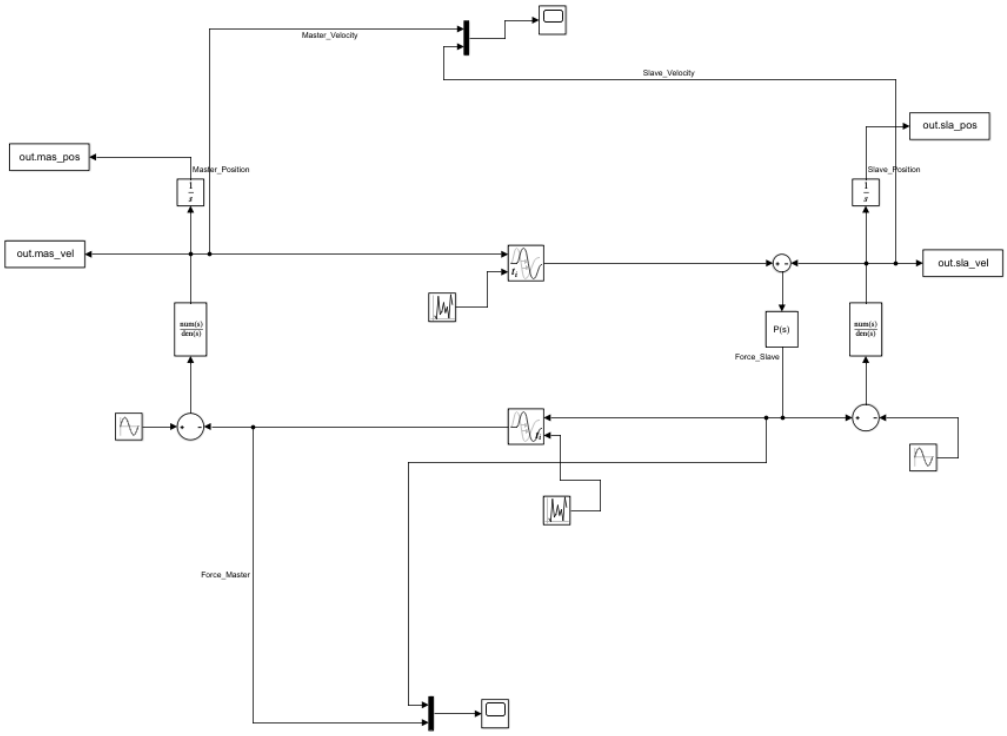

Figure 4.9: Simulink model of the current controller

Proposed controller

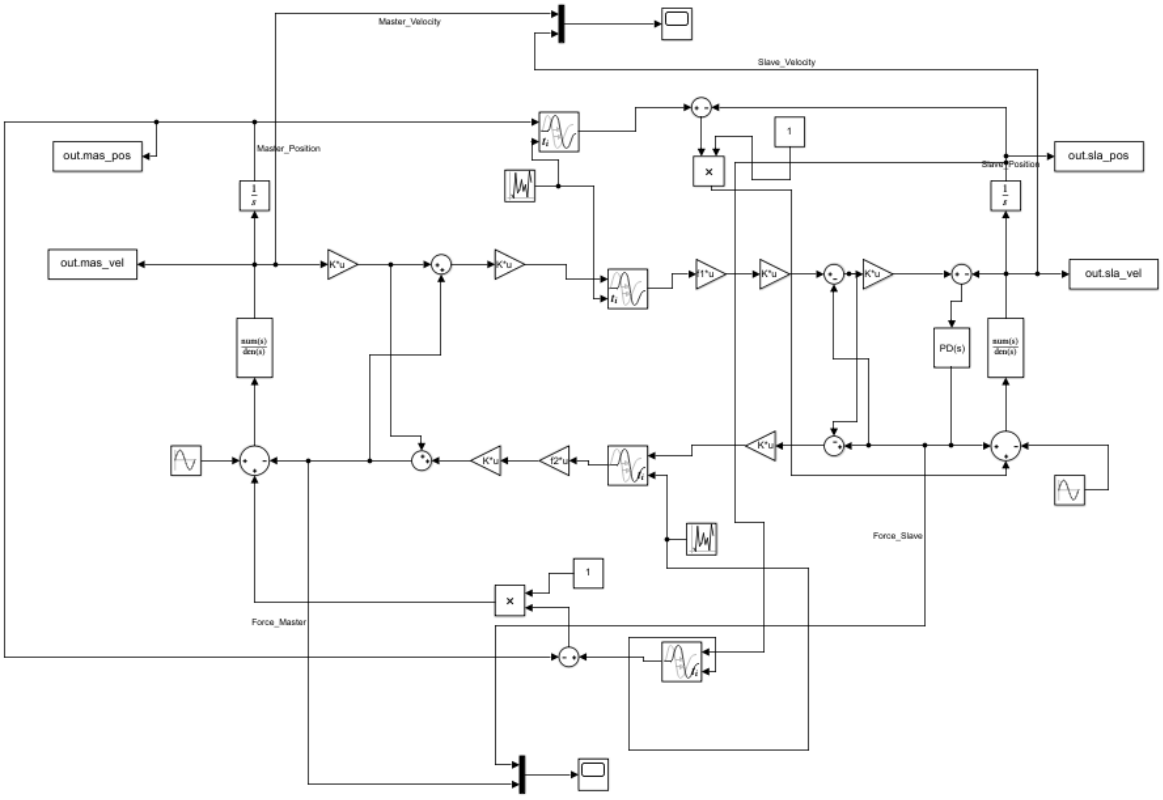

Figure 4.10: Simulink model of the proposed controller

Chapter 5

Experiments and Results

In this chapter will the performed experiments and the results gathered from the experiments be showcased and discussed. The main motivation for conducting the experiments was to evaluate the performance of the proposed control architecture in terms of its capability of handling the effects of time-delay and to compare its performance against that of the current control architecture. The desired outcome when using a bilateral tele-operation system is to have the slave behave in the same manner as the master with respect to the power variables *velocity*, *force*, and *position*. To test the performance of the controllers in such regard, the Simulink model from previous chapter were used. There was sent sine wave signals between master and slave site, representing master velocity and slave force. The velocity was sent from master to slave site and the force from slave to master site, with added time-delay to the system. To evaluate the controllers performance, the signals was examined before and after being received at their respective site by checking whether the system was able to maintain their quality and deliver them without delay while sustaining the stability of the system. The controllers were tested with time-delay of value: 0, 200, 400, and 600 ms, both in case of constant and varying time-delay.

In regards to the tuning parameters of the proposed controller, their values were set to:

1. $K_{fed} = 1$
2. $b = 2$

To separate the two controllers from each other in an understandable manner, they will in the following sections be referred to as *controller-a*

(proposed controller) and *controller-b* (current controller). Furthermore, *velocity_master* and *velocity_slave* in the figures will represent $\dot{x}_m$ and $\dot{x}_s$ respectively, while *master_force* and *slave_force* represents f_m and f_s from figure 4.6.

5.1 Constant time-delay

As the controllers in this section of the chapter will deal with constant time-delay, it was by Chopra *et al.* recommended to set the varying gains $f_i = 1$ in the case of constant time-delay [22].

5.1.1 Case 1: $T = 0$ ms

Controller-a:

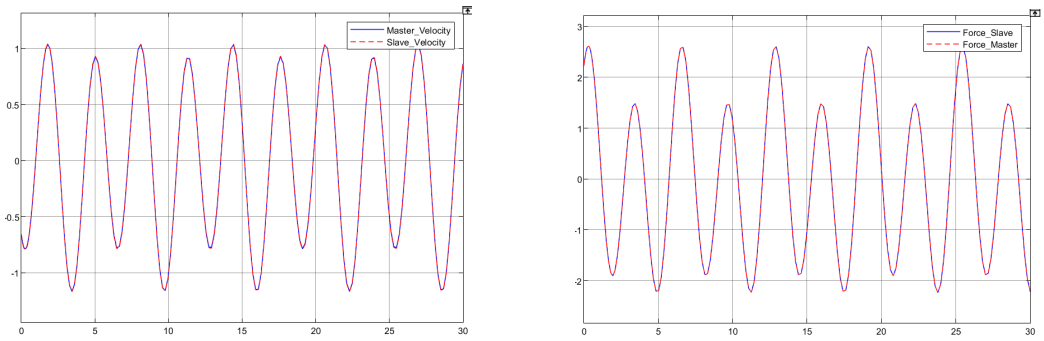

(a) Velocity (b) Force

Figure 5.1: Velocity and force results with constant delay = 0 ms

Controller-b:

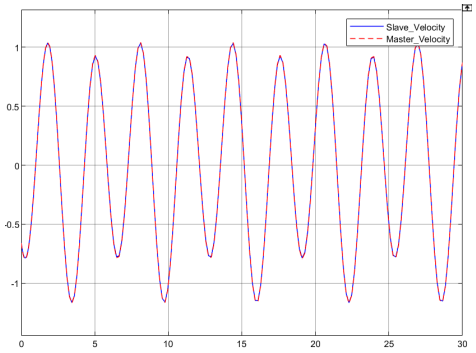

(a) Velocity

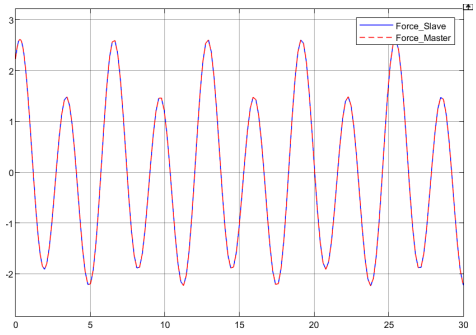

(b) Force

Figure 5.2: Velocity and force results with constant delay = 0 ms

5.1.2 Case 2: $T = 200$ ms

Controller-a:

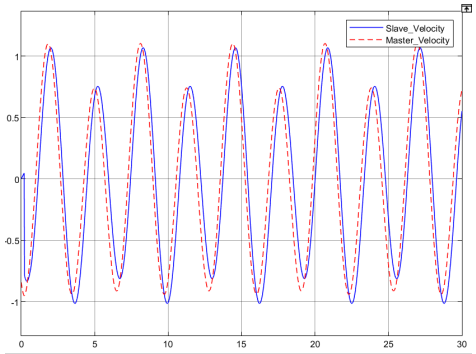

(a) Velocity

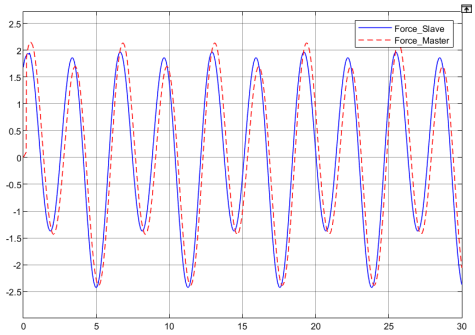

(b) Force

Figure 5.3: Velocity and force results with constant delay = 200 ms

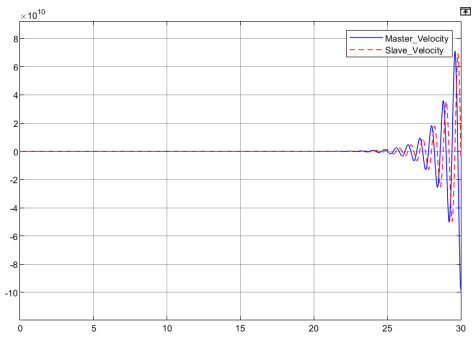

(a) Velocity

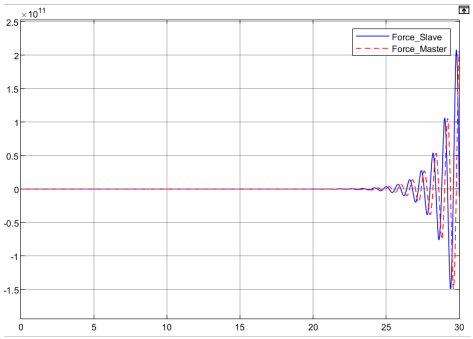

(b) Force

Figure 5.4: Velocity and force results with constant delay = 200 ms

Controller-b:

5.1.3 Case 3: $T = 400$ ms

Controller-a:

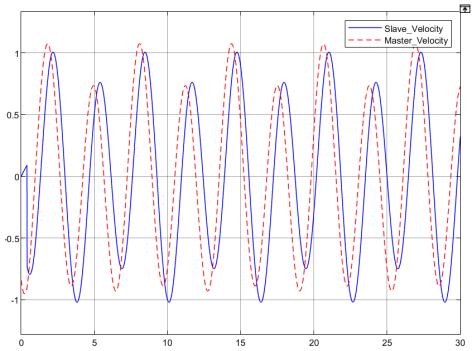

(a) Velocity

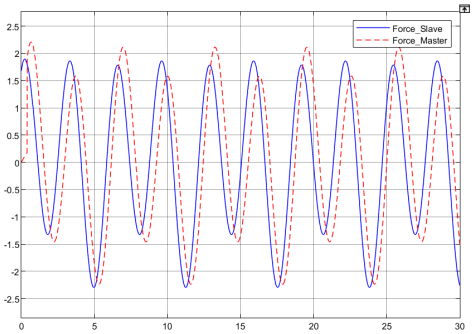

(b) Force

Figure 5.5: Velocity and force results with constant delay = 400 ms

Controller-b:

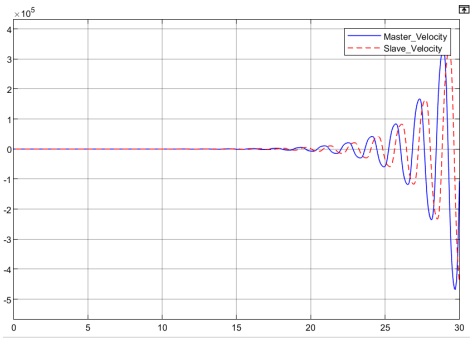

(a) Velocity

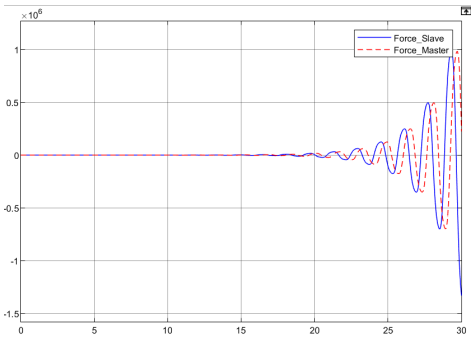

(b) Force

Figure 5.6: Velocity and force results with constant delay = 400 ms

5.1.4 Case 4: $T = 600$ ms

Controller-a:

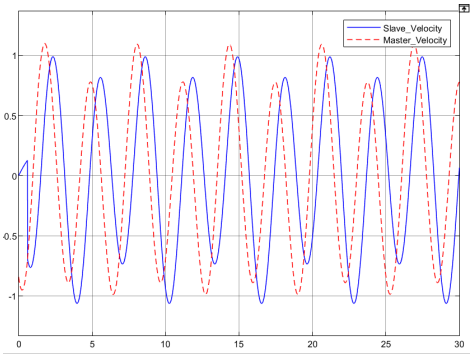

(a) Velocity

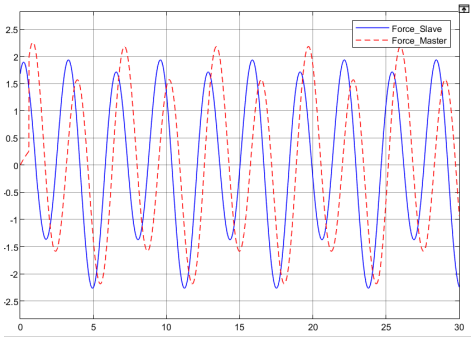

(b) Force

Figure 5.7: Velocity and force results with constant delay = 600 ms

Controller-b:

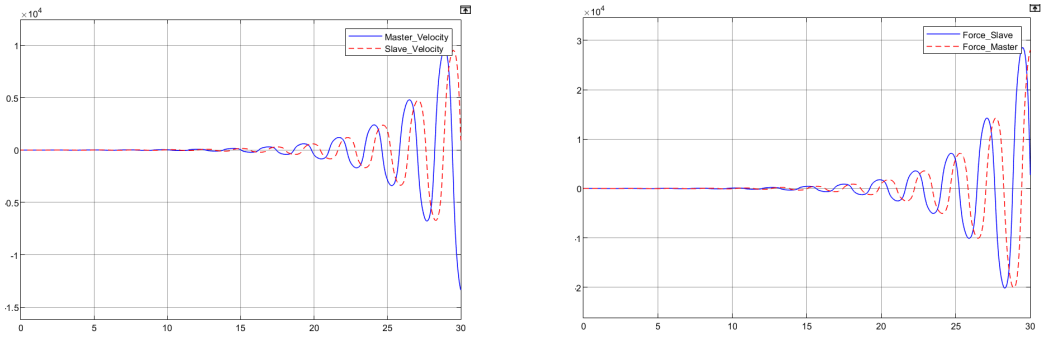

(a) Velocity (b) Force

Figure 5.8: Velocity and force results with constant delay = 600 ms

As previously mentioned in this section, the results will be defined as desirable in the cases where the stability of the system has been maintained, the quality of the power variables (velocity and force) has been preserved and they have been delivered to their set destination without any delay.

1. **Controller-a:** It can for the results of controller-a be seen that it for all the tested values of T in case of constant time-delay was able to maintain the stability of the system. It can also be noted that the results was found to be most desirable for T = 200 ms, where the controller was both able to maintain the quality of the power variables and deliver them to their respective sites without any noticeable delay. But as the value of T was increased, the arrival time of the power variables similarly got increased and their quality also slightly decreased.

2. **Controller-b:** For controller-b it can be noticed that it was able to produce desirable results for T = 0 ms, but as time-delay was added to the system it was not able to handle its effects and the system became unstable rather quickly.

5.2 Varying time-delay

For the cases where the controls were tested with varying-time delay it was for controller-a decided to set the varying gains $f_i = 0.9$. The value was chosen after testing the system with different values to determine the value that would suit the system the most in terms of increasing its overall performance.

5.2.1 Case 1: $T \leq 200$ ms:

Controller-a:

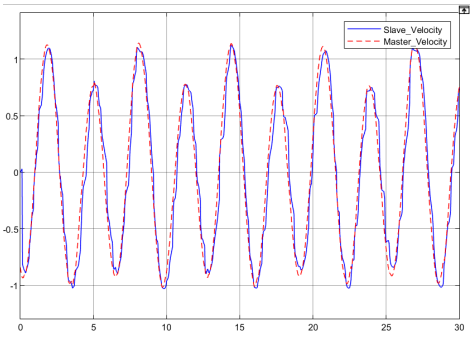

(a) Velocity

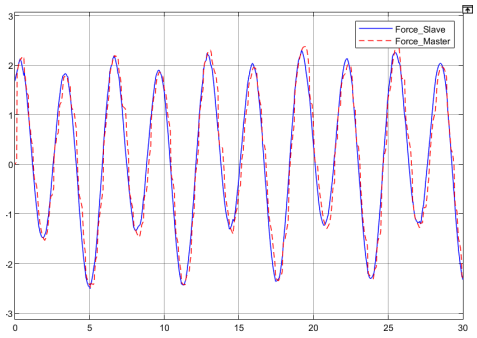

(b) Force

Figure 5.9: Velocity and force results with varying time delay ≤ 200 ms

Controller-b:

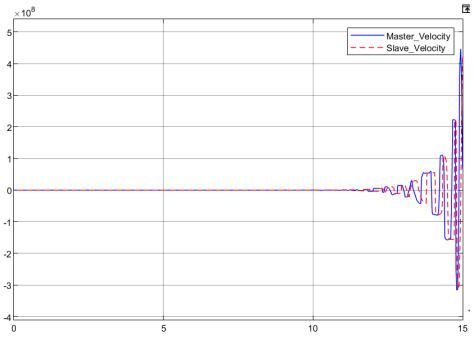

(a) Velocity

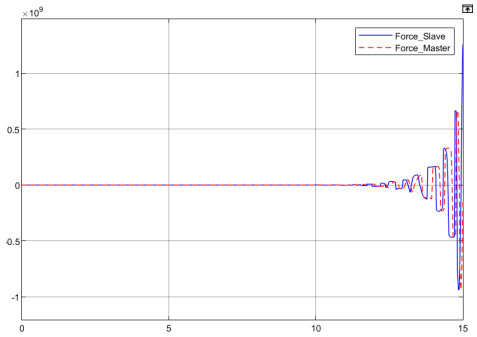

(b) Force

Figure 5.10: Velocity and force results with varying time delay ≤ 200 ms

5.2.2 Case 2: $T \leq 400$ ms:

Controller-a:

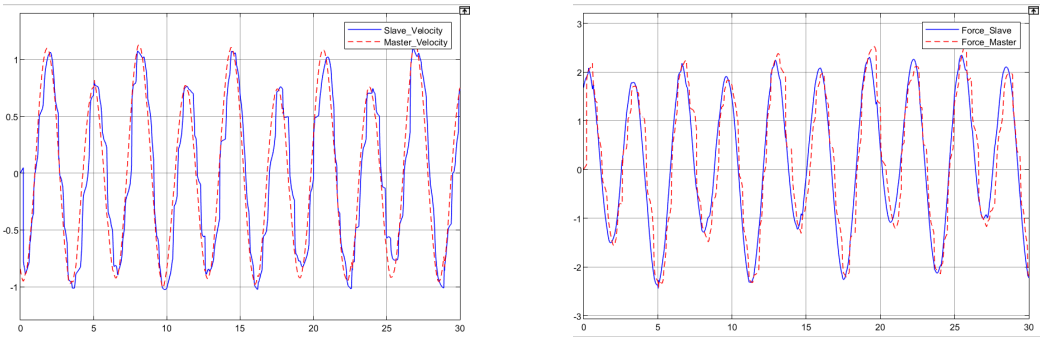

(a) Velocity (b) Force

Figure 5.11: Velocity and force results with varying time delay ≤ 400 ms

Controller-b:

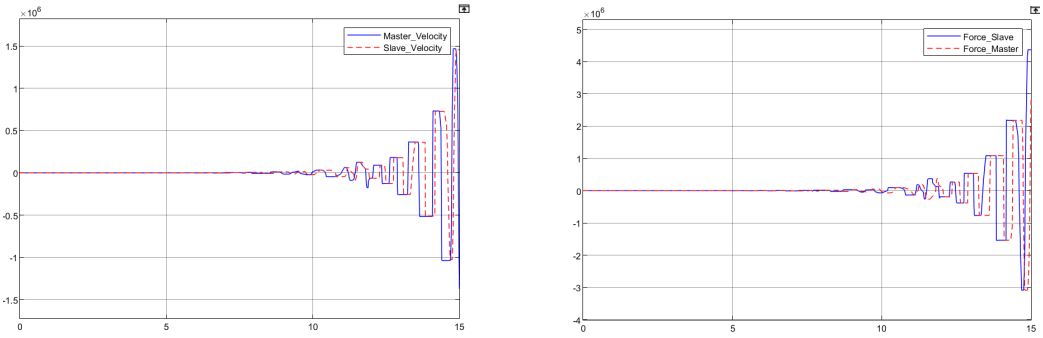

(a) Velocity (b) Force

Figure 5.12: Velocity and force results with varying time delay ≤ 400 ms

5.2.3 Case 3: $T \leq 600$ ms:

Controller-a:

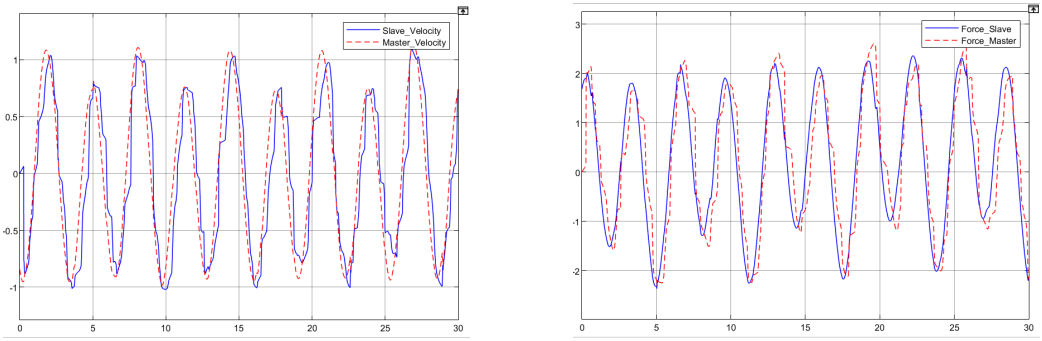

(a) Velocity (b) Force

Figure 5.13: Velocity and force results with varying time delay ≤ 600 ms

Controller-b:

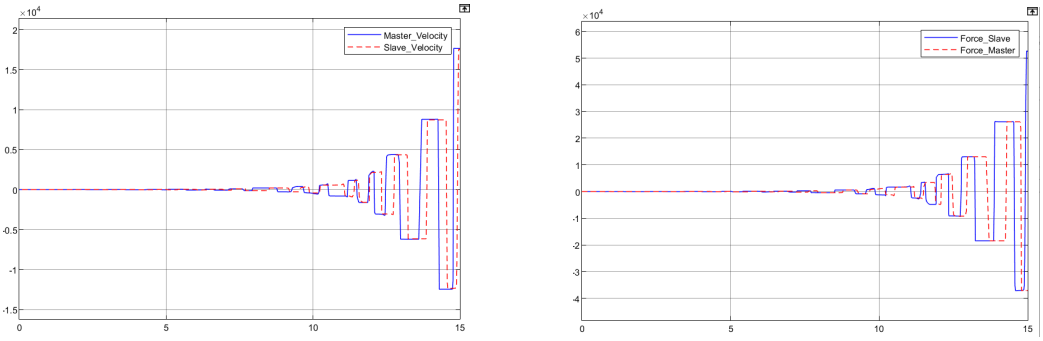

(a) Velocity (b) Force

Figure 5.14: Velocity and force results with varying time delay ≤ 600 ms

1. **Controller-a:** It can for controller-a be seen that it for all the tested cases was able to produce good results. The stability was preserved in for each of the time-delay values, the quality of the power variables was mostly kept with a slight decrease as the time-delay value was increased, and the delay did not have any noticeable impact on the arrival time of the power variables.

2. **Controller-b:** Similarly to the results found in the case of constant time-delay, it can be seen that controller-b was not able to handle varying time-delay either, as the system ones again became unstable.

5.2.4 Tuning of wave impedance value

There will be a need to tune the wave impedance parameter when taking into use the wave variable method and based on how the parameter is tuned, its value may have an noticeable impact on the systems overall performance. There was in this work performed simulations, using the Simulink model of the proposed control architecture, to determine the impact that the value of the wave impedance may have on the system. The value of the wave impedance and other tuning parameters of the controller were set to:

1. $T = 100$ ms
2. $K_{fed} = 1$
3. $b = 0.1$, 3, 10 and 50

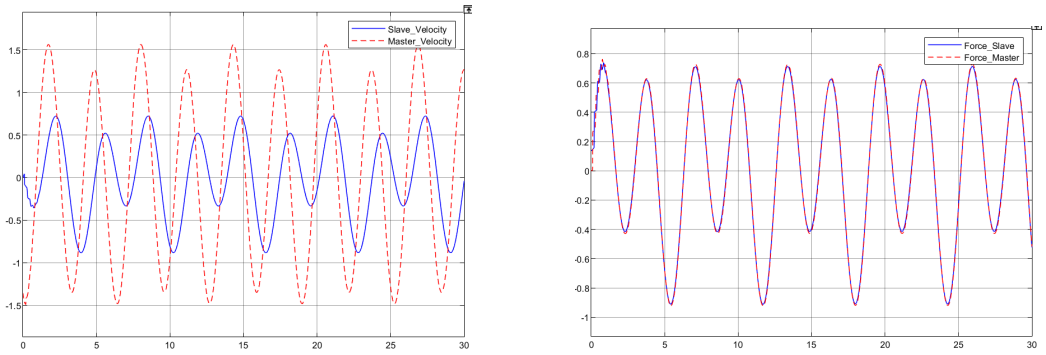

(a) Velocity (b) Force

Figure 5.15: Velocity and force with b = 0.1

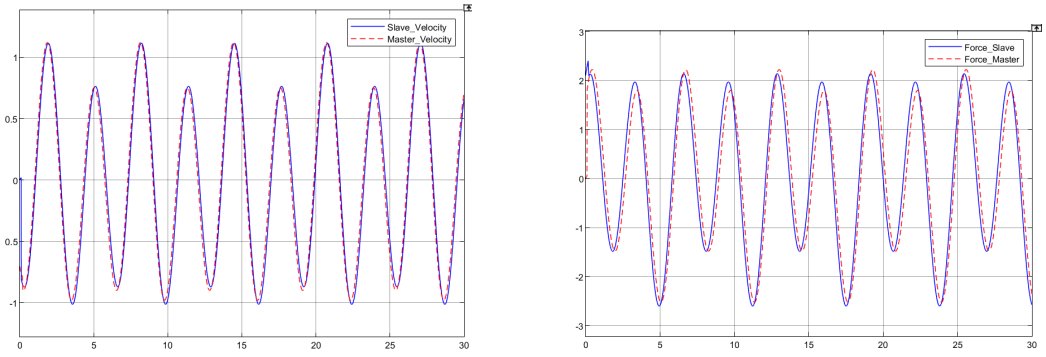

(a) Velocity (b) Force

Figure 5.16: Velocity and force with b = 3

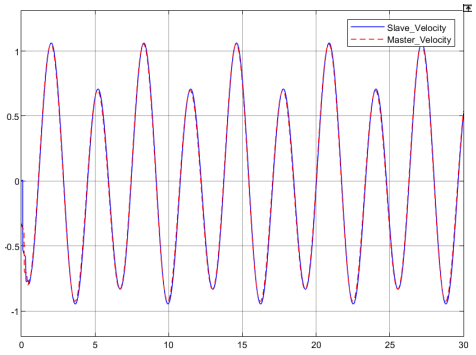

(a) Velocity

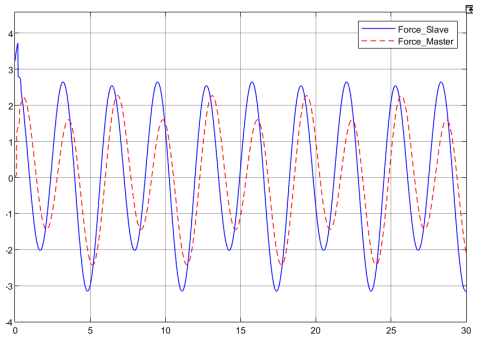

(b) Force

Figure 5.17: Velocity and force with b = 10

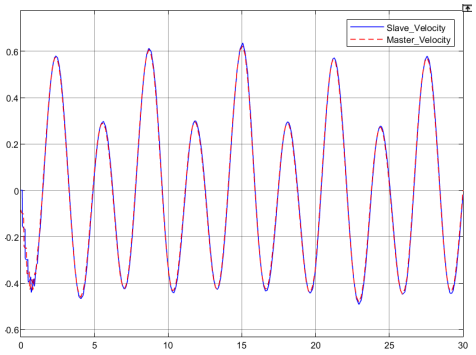

(a) Velocity

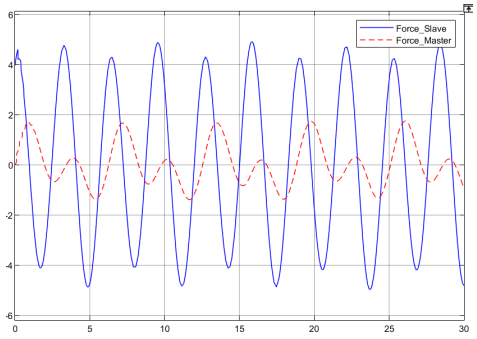

(b) Force

Figure 5.18: Velocity and force with b = 50

The results gathered from the performed simulation can be seen in figure 5.13 - 5.16. It can from the figures be seen that when tested with a low wave impedance value, b = 0.1, the system was able to produce relative good results for the force, but the velocity results with such low value was not found to be desirable. As the value of the wave impedance was increased it can be noted that that it caused the force results to degrade while the quality of the velocity results improved. Based upon these results it can be concluded with that the value of the wave impedance parameter will have an substantial impact on the overall performance of the system. It is therefore important that its value is tuned and set to a midpoint value that will allow the system to produce overall sufficient results. For the system used to simulate in this work it would be befitting to set the wave impedance parameter to a value between 2 and 3.

Chapter 6

Discussion

6.1 Gathered results

Regarding the findings in this work, it is important to mention that they only are applicable for systems of 1-DoF and under ideal circumstances, as both the current and proposed control architectures were simulated and tested using simplified 1-DoF Simulink models without real-world factors such as noise being included. Meanwhile, the setup at the Intervention Center is a multi-DoF system and there will be noise occurring during its use, therefore will the results from this work only be an indication of how well the proposed control architecture may work in the real-world.

Based on the results in chapter 5, it can be seen that the system when using the current control architecture and time-delay set to T = 0 ms was able to produce desirable results, but as time-delay was added to the system it no longer was able to maintain its stability. The reason for the destabilization is due to the fact that the system contains force-reflection and as previously mentioned, systems with force-reflection when dealing with time-delay will become destabilized. Since the current control architecture primarily was designed for a system that would be used to perform ultrasound examinations locally without any noticeable time-delay, the issue of force-reflection with time-delay was not taken into consideration during the design of the control architecture and thus the system was not able to handle time-delay with, becoming destabilized.

Meanwhile when tested with the proposed control architecture, the system was for all the cases able to maintain its stability. The reason for change in behaviour is due to the implementation of the wave variable method. The wave variable method, as previously mentioned, is a control strategy that was designed with the purpose of sustaining the stability of a system with

force-reflection when dealing with time-delay. It can also for the proposed control architecture be noted that the results were found to be more desirable in the case of varying time-delay. The difference in results is due to mainly two reasons. As mentioned in section 2.1.3, there has in the recent years been a change in the type of communication network that is used to establish the link between master and slave site, where it now is common to use Internet based networks. There will with such network be caused varying time-delay during the communication between the sites, for that reason and due to the fact that the Intervention Center is planning to extend their setup with 5G it was found to beneficial to design the control architecture with the ability to handle both constant and varying time-delay, but mainly varying time-delay. Another reason for the difference in results is because of the *random number* block that was used with the Simulink model for varying time-delay. The block produces a random number between an interval and since the numbers will be random it will in some cases cause the delay to be lower than the set max value of the interval. For example, if the max value is set to 600 ms there will be generated numbers lower than that value for varying time-delay, while for constant time-delay the time-delay value will have a constant value of 600 ms, which will result in the time-delay being higher in case of constant time-delay.

It is also, regarding Internet based networks, important the the proposed controller is able to produce desirable results in case of packet loss and jitter. There has not been performed any experiments in this work regarding these parameters and their potential effects on the system, but concerning the issue of packet loss it was by Chopra *et al.*, using a similar control architecture, performed experiments to determine the controllers ability to handle packet loss. The system was tested with 0, 20, 50 and 80% packet loss and the research was concluded with the system, for all tested cases, being able to maintain the stability of the system due to the implemented feedback and feed-forward controller, but as the values of the packet loss was increased the tracking performance of the system was degraded [6]. Based on the findings of that research it can be assumed that the proposed control architecture similarly will allow the system to handle packet loss in a sufficient manner.

There has from previous done work in the field of tele-operation not been conducted any noticeable research to determine the wave variable method's ability to handle jitter. A solution to handle jitter can be to separate the packet from each other using either time-stamps or numbers, resulting in the packets being delivered in correct order, but this will in hindsight increase the delay in the system since a buffer will be used. It is therefore important that jitter, together with packet loss, is looked further into in future work to determine the proposed controller's ability of handling their effects.

As there has been proven in this work, time-delay will have an substantial impact on a tele-operational system's behavior, especially for systems with force-reflection as time-delay will cause the system to destabilize. It is therefore important to take into use a control strategy that will minimize the effects of time-delay. Based on gathered results in this and previously done work, it can be seen that the wave variable method is an efficient and reliable method to use against time-delay. It ensures stability in case of delayed bilateral system, is easy to implement into existing control schemes without having to design a new one from scratch, can be modified to receive more accurate results in terms of tracking performances and consists of only few tuning parameters that can be tuned to improve the overall performance of the system without destabilizing it. The only noticeable drawback to the method is that when used on its own, without any added modifications, it will not be able to produce satisfactory tracking performance results or sustain the systems stability in case of varying time-delay, but as mentioned, such issues can be resolved by modifying the method further.

It is important to ensure that the proposed controller will allow the system to perform sufficiently while being able to handle the amount of time-delay that remote ultrasound examinations are performed with. As previously mentioned, it was by Song Xu *et al.* recommended to only perform tele-surgery procedures when the time-delay is $T \leq 200$ ms [41]. By comparing the results of the proposed controller for $T = 200$ ms with the statement of Song Xu, it can be assumed that the proposed controller would be a suitable controller to use for remote ultrasound examination, as it for the relevant time-delay value was able to produce adequate results in both case of constant and varying time-delay.

6.2 5G as potential communication network

It is planned to extend the setup at the Intervention Center by using 5G as the communication network to establish the link between master and slave site, thus allowing for remote use of the setup. As mentioned, the communication network that is used will have an substantial impact on the behaviour and performance of system. It is therefore important to ensure that 5G is a suitable communication network to use when performing remote ultrasound examinations. As described in section 2.2, 5G is the latest and improved version of wireless mobile network. It is, due to its low latency, great bandwidth and speed, a communication network that in recent years has been frequently used as the medium for tele-operation systems. Also mentioned in section 2.1, there are certain requirements that the communication network has to

meet to ensure real-time performance during an remote ultrasound examination with force-feedback. Together with the performance requirements it is also important to verify that the communication network allows for examinations to be performed on patients located at remote areas, as it is one of the main premises of taking into use a tele-echography system. To verify 5G as a suitable communication network can findings of previously done work be looked into, such as the research of Wei Tian *et al.* who tested their tele-surgery using 5G with distances of 120, 280, 750, 1200, and 3000 km and conclude their research with the system being able to produce accurate and reliable results due to 5G [35] or the work of Shaobo Duan *et al.* who concluded their work with saying that using 5G led to clear images, safe procedure, and gave a sensation of performing bedside examination [9]. Using these findings and that of what has previously been presented in this work in terms of 5G's capabilities, it can be established that 5G is an efficient and reliable communication network and using it with the setup at the Intervention Center to perform remote examinations will lead to efficient, safe and accurate performances.

Chapter 7

Future work

7.1 Implementations

There was in this work, due to lack of necessary equipment, performed simulations using simplified 1-DoF models of both the current and proposed controller to test their performance when having to deal with time-delay. During the simulations real-world factors such as noise was neglected, thus resulting in the simulations producing results that only are applicable for 1-DoF systems and obtainable under ideal circumstances. As it has been mentioned in this work, when using the real multi-DoF system there will be an occurrence of noise and therefore should the next step to improve be proposed solution be to implement the proposed controller with the setup at the Intervention Center such that more realistic results can be produced.

Following the implementation of the proposed controller, it will be beneficial to conduct different experiments. The premise of the experiments should be to ensure the findings in this work. To confirm the findings, there can be performed similar tests of those in chapter 5, by sending velocity and force measurements between master and slave with added time delay to the system and thereafter examining the findings to confirm that they are desirable. Another aspect of the experiments should be to verify the capability of the system in terms of its control performance during an remote ultrasound examination.

As mentioned, there was during this work not looked into the proposed controller's capability of dealing with jitter and packet loss, therefore should there also be conducted experiments to ensure that the system will be able to handle their effects while producing sufficient results.

Chapter 8

Conclusion

In this work, the effect of time-delay on tele-operational system has been looked into and a control architecture has been proposed to limit the effects of time-delay, allowing for remote ultrasound examinations to be performed without time-delay being an hindrance. Tele-echography systems take into use force-feedback to give the sonographer the sensation of controlling the slave-environment directly, thus giving them more information to rely on during the examination. However, the slightest time-delay will cause such system to destabilize. To combat this issue, there exists different control strategies that can be implemented. In this work, the wave variable method was taken into use. The wave variable method is a method that primarily was designed to sustain the stability of a delayed bilateral system, but from previously done work it has been shown that using wave variable method leads to poor tracking performance and causes the system to destabilize in case of varying time-delay. To bypass the weaknesses of the wave variable method, it was in this work chosen to use the suggestions of Chopra *et al.*, they advised to implement a feed-forward and feedback controller to increase the performance of the system when using the wave variable method and a varying gain f_i to maintain its stability when dealing with varying time-delay [6]. These suggestions, together with the wave variable method, were used to extend the current control architecture, thus creating the proposed control architecture. To test the ability of both the current and proposed control architecture's ability to handle effects of time delay, there was created a simplified 1-DoF Simulink model for both of control architectures. The models were used to perform simulations with added time-delay of values 200, 400, and 600 ms. The results of the performed simulations were found to match that of the theory and findings from previously done work, as using the current control architecture led the system to became unstable. The instability was caused due to the design of the current controller, as it

has not been designed to handle the effects that time-delay will have on a bilateral system. Meanwhile, the results when using the proposed control architecture were found to be sufficient, as the system was able to maintain its stability for all the tested time-delay values, both in case of constant and varying time-delay. The results were especially found to be desirable for T = 200 ms, which is the maximum amount of time-delay it is recommended to perform tele-operational procedures with, thus giving an indication on how well results the setup at the Intervention Center might produce when using the proposed control architecture. However, as the findings in this work only are applicable for 1-DoF models and real-world factors such as noise were not taken into consideration, it will be necessary to implement and test the proposed controller with the setup at the Intervention Center, to both receive more realistic results and to ensure the findings in this work are obtainable in a real-world scenario.

Additionally, the mobile network 5G was researched and evaluated in terms of its capabilities and potential to be used as the medium for for the setup at the Intervention Center, allowing for remote use. To be a suitable communication network for tele-echography and allow for real-time performance, the performance rate of the network has to meet certain requirements in regards to parameters such as latency and bandwidth. Having looked into both the performance capabilities of 5G and the findings of previously done work in regards to use of 5G for tele-operation, it could be concluded with 5G meeting the necessary requirements, thus being a efficient and reliable network to use for tele-echography.

Bibliography

[1] Marc T Alise. Expansion and implementation of the wave variable method in multiple degree-of-freedom systems. 2007.

[2] R.J. Anderson and M.W. Spong. Bilateral control of teleoperators with time delay. In *Proceedings of the 1988 IEEE International Conference on Systems, Man, and Cybernetics*, volume 1, pages 131–138, 1988.

[3] Philippe Arbeille, Arnaud Capri, Jean Ayoub, Veronique Kieffer, Monica Georgescu, and Gerard Poisson. Use of a robotic arm to perform remote abdominal telesonography. *American journal of Roentgenology*, 188(4):W317–W322, 2007.

[4] S. Avgousti, E. Christoforou, Andreas S. Panayides, S. Voskarides, C. Novales, L. Nouaille, C. Pattichis, and P. Vieyres. Medical telerobotic systems: current status and future trends. *BioMedical Engineering OnLine*, 15, 2016.

[5] Hangjun Chen, Yibo Zhou, Fuhua Chen, Lei Xu, Yinru Li, and Liping Zhou. Clinical value of 5g-based robotic tele-ultrasound system in quarantined patients with coronavirus disease 2019. *Chinese Journal of Medical Ultrasound (Electronic Edition)*, 17(10):1021, 2020.

[6] Nikhil Chopra, Mark W Spong, Romeo Ortega, and Nikita E Barabanov. On tracking performance in bilateral teleoperation. *IEEE Transactions on Robotics*, 22(4):861–866, 2006.

[7] Fabien Courreges, Pierre Vieyres, and RSH Istepanian. Advances in robotic tele-echography services-the otelo system. In *The 26th Annual International Conference of the IEEE Engineering in Medicine and Biology Society*, volume 2, pages 5371–5374. IEEE, 2004.

[8] Mehmet Dede and Sabri Tosunoglu. Fault-tolerant teleoperation systems design. *Industrial Robot: An International Journal*, 2006.

[9] Shaobo Duan, Luwen Liu, Yongqing Chen, Long Yang, Ye Zhang, Shuaiyang Wang, Liuwei Hao, and Lianzhong Zhang. A 5g-powered robot-assisted teleultrasound diagnostic system in an intensive care unit. *Critical Care*, 25(1):1–9, 2021.

[10] Terence Essomba, Laurence Nouaille, MA Laribi, G Poisson, and S Zeghloul. Design process of a robotized tele-echography system. In *Applied Mechanics and Materials*, volume 162, pages 384–393. Trans Tech Publ, 2012.

[11] Jørgen Enger Fjellin. Design of a bilateral master-slave system with haptic feedback for ultrasound examinations. Master's thesis, 2013.

[12] C. Geng, Q. Xie, L. Chen, A. Li, and B. Qin. Study and analysis of a remote robot-assisted ultrasound imaging system. In *2020 IEEE 4th Information Technology, Networking, Electronic and Automation Control Conference (ITNEC)*, volume 1, pages 389–393, 2020.

[13] Chuan Geng, Qiang Xie, Long Chen, Alex Li, and Binjie Qin. Study and analysis of a remote robot-assisted ultrasound imaging system. In *2020 IEEE 4th Information Technology, Networking, Electronic and Automation Control Conference (ITNEC)*, volume 1, pages 389–393. IEEE, 2020.

[14] Petro Griffa, Alessandro Filippeschi, and Carlo Alberto Avizzano. Kinematic optimization for the design of a ur5 robot end-effector for cardiac tele-ultrasonography. In *The International Conference of IFToMM ITALY*, pages 423–430. Springer, 2020.

[15] Gwang Min Gu, DongJu Lee, and Jung Kim. Development of a low cost force sensor for wearable robotic systems. In *2011 IEEE International Conference on Robotics and Biomimetics*, pages 1450–1455. IEEE, 2011.

[16] A. Gupta and R. K. Jha. A survey of 5g network: Architecture and emerging technologies. *IEEE Access*, 3:1206–1232, 2015.

[17] Blake Hannaford and Allison M Okamura. Haptics. In *Springer Handbook of Robotics*, pages 1063–1084. Springer, 2016.

[18] Peter F Hokayem and Mark W Spong. Bilateral teleoperation: An historical survey. *Automatica*, 42(12):2035–2057, 2006.

[19] Keiichiro Ito, Koichi Tsuruta, Shigeki Sugano, and Hiroyasu Iwata. Evaluation of a wearable tele-echography robot system: Fastele in a vehicle

using a mobile network. In *2011 Annual International Conference of the IEEE Engineering in Medicine and Biology Society*, pages 2093–2096. IEEE, 2011.

[20] Olga Kostyukova, Felipe P Vista IV, and Kil To Chong. Design of feed-forward and feedback position control for passive bilateral teleoperation with delays. *ISA transactions*, 85:200–213, 2019.

[21] Guanyang LIU, Xuda GENG, Lingzhi LIU, and Yan WANG. Haptic based teleoperation with master-slave motion mapping and haptic rendering for space exploration. *Chinese Journal of Aeronautics*, 32(3):723 – 736, 2019.

[22] Regelio Lozano, Nikhil Chopra, and Mark W Spong. Passivation of force reflecting bilateral teleoperators with time varying delay. In *Proceedings of the 8. Mechatronics Forum*, number 954-962, pages 24–26, 2002.

[23] Dewanand A Meshram and Dipti D Patil. 5g enabled tactile internet for tele-robotic surgery. *Procedia Computer Science*, 171:2618–2625, 2020.

[24] Georgios Minopoulos, Georgios Kokkonis, Konstantinos Psannis, and Yutaka Ishibashi. A survey on haptic data over 5g networks. 2019.

[25] Becky Morton and Penny Delf. The prevalence and causes of msi amongst sonographers. *Radiography*, 14(3):195–200, 2008.

[26] Saghir Munir and Wayne J Book. Internet based teleoperation using wave variables with prediction. In *2001 IEEE/ASME International Conference on Advanced Intelligent Mechatronics. Proceedings (Cat. No. 01TH8556)*, volume 1, pages 43–50. IEEE, 2001.

[27] Edvard Naerum and Blake Hannaford. Global transparency analysis of the lawrence teleoperator architecture. In *2009 IEEE International Conference on Robotics and Automation*, pages 4344–4349. IEEE, 2009.

[28] Günter Niemeyer and J-JE Slotine. Stable adaptive teleoperation. *IEEE Journal of oceanic engineering*, 16(1):152–162, 1991.

[29] Laurence Nouaille, Natalie Smith-Guérin, Gérard Poisson, and Philippe Arbeille. Optimization of a 4 dof tele-echography robot. In *2010 IEEE/RSJ International Conference on Intelligent Robots and Systems*, pages 3501–3506. IEEE, 2010.

[30] Ilia G Polushin, Abdelhamid Tayebi, and Horacio J Marquez. Stabilization scheme for force reflecting teleoperation with time-varying communication delay based on ios small gain theorem. *IFAC Proceedings Volumes*, 38(1):394–399, 2005.

[31] Juan Sandoval, Med Amine Laribi, Said Zeghloul, and Marc Arsicault. Towards a safe physical human-robot interaction for tele-operated system: application to doppler sonography. In *IFToMM Symposium on Mechanism Design for Robotics*, pages 335–343. Springer, 2018.

[32] J. Seo, J. H. Cho, M. W. Lee, T. Kim, H. Par, S. Kim, C. Kim, and O. Kwon. Feasibility evaluation of mobile internet based robot-assisted tele-echography system. In *2018 15th International Conference on Ubiquitous Robots (UR)*, pages 53–56, 2018.

[33] Joonho Seo, Jang Ho Cho, Juyoung Cha, Changwon Kim, and Ohwon Kwon. Design and experimental evaluations of robot-assisted tele-echography system for remote ultrasound imaging. In *2017 14th International Conference on Ubiquitous Robots and Ambient Intelligence (URAI)*, pages 592–594. IEEE, 2017.

[34] Alejandro Jarillo Silva, Omar A Domínguez Ramirez, Vicente Parra Vega, and Jesus P Ordaz Oliver. Phantom omni haptic device: Kinematic and manipulability. In *2009 Electronics, Robotics and Automotive Mechanics Conference (CERMA)*, pages 193–198. IEEE, 2009.

[35] Wei Tian, Mingxing Fan, Cheng Zeng, Yajun Liu, Da He, and Qi Zhang. Telerobotic spinal surgery based on 5g network: the first 12 cases. *Neurospine*, 17(1):114, 2020.

[36] Pierre Vieyres, Laurence Josserand, Marco Chiccoli, Juan Sandoval, Nicolas Morette, Cyril Novales, Aicha Fonte, Soteris Avgousti, Sotos Voskarides, and Takis Kasparis. A predictive control approach and interactive gui to enhance distal environment rendering during robotized tele-echography: Interactive platform for robotized telechography. In *2012 IEEE 12th International Conference on Bioinformatics & Bioengineering (BIBE)*, pages 233–239. IEEE, 2012.

[37] Pierre Vieyres, Gérard Poisson, Fabien Courrèges, Olivier Mérigeaux, and Philippe Arbeille. The teresa project: from space research to ground tele-echography. *Industrial robot: an international journal*, 2003.

[38] Pierre Vieyres, Gérard Poisson, Fabien Courrèges, Natalie Smith-Guerin, Cyril Novales, and Philippe Arbeille. A tele-operated robotic

system for mobile tele-echography: The otelo project. In *M-health*, pages 461–473. Springer, 2006.

[39] Adriana Vilchis, Jocelyne Troccaz, Philippe Cinquin, Kohji Masuda, and Franck Pellissier. A new robot architecture for tele-echography. *IEEE Transactions on Robotics and Automation*, 19(5):922–926, 2003.

[40] Jing Wang, Chengzhong Peng, Yan Zhao, Ruizhong Ye, Jun Hong, Haijun Huang, and Legao Chen. Application of a robotic tele-echography system for covid-19 pneumonia. *Journal of Ultrasound in Medicine*, 40(2):385–390, 2021.

[41] Song Xu, Manuela Perez, Kun Yang, Cyril Perrenot, Jacques Felblinger, and Jacques Hubert. Determination of the latency effects on surgical performance and the acceptable latency levels in telesurgery using the dv-trainer® simulator. *Surgical endoscopy*, 28(9):2569–2576, 2014.

[42] Ruizhong Ye, Xianlong Zhou, Fei Shao, Linfei Xiong, Jun Hong, Haijun Huang, Weiwei Tong, Jing Wang, Shuangxi Chen, Ailin Cui, et al. Feasibility of a 5g-based robot-assisted remote ultrasound system for cardiopulmonary assessment of patients with coronavirus disease 2019. *Chest*, 159(1):270–281, 2021.

[43] CJ Zandsteeg, DJH Bruijnen, and MJG Van de Molengraft. Haptic teleoperation system control design for the ultrasound task: A loop-shaping approach. *Mechatronics*, 20(7):767–777, 2010.

[44] Jiayi Zhu, Xiaochuan He, and Wail Gueaieb. Trends in the control schemes for bilateral teleoperation with time delay. In *International Conference on Autonomous and Intelligent Systems*, pages 146–155. Springer, 2011.